Int J Earth Sci (Geol Rundsch) (2003) 92:852–872
DOI 10.1007/s00531-003-0356-5

ORIGINAL PAPER

Sofia De Gregorio · Silvio G. Rotolo · Igor M. Villa

Geochronology of the medium to high-grade metamorphic units of the Peloritani Mts., Sicily

Received: 3 March 2003 / Accepted: 27 June 2003 / Published online: 14 November 2003
© Springer-Verlag 2003

Abstract The Peloritani Mountains are a fragment of an orogen variably attributed to the Alpine or Hercynian orogeny. On the basis of ^{39}Ar-^{40}Ar, U-Pb and Rb-Sr dating, the main metamorphism of the two medium–high grade metamorphic units, the Mela and Aspromonte Units, and most of the thrusting responsible for stacking the orogenic edifice are seen to be Hercynian. The main thrusting of the Aspromonte Unit over the lower grade units took place at 301±2 Ma. Brittle deformation during Tertiary reactivation of Hercynian thrust planes did not generate any rejuvenation of white micas in the studied sector. Our dataset shows a great complexity and we propose to unravel it by considering different levels of information. To first order, the Mela and Aspromonte Units differ in their metamorphic paths and their geochronological evolution. The Mela Unit shows generally younger ages (Carboniferous) than the Aspromonte Unit and, unlike the latter, was extensively retrogressed in greenschist facies. The Aspromonte Unit is itself geochronologically heterogeneous. Proterozoic ages are preserved both in titanite and in amphibole relics of one tectonic subunit; Devonian to Carboniferous amphibole ages are found in different other subunits; tertiary overprint is minor and spatially limited. We propose to consider the chronologically heterogeneous subunits as accreted pre-Hercynian terranes amalgamated late during the Hercynian orogeny. Micas in both units give scattered Mesozoic ^{39}Ar-^{40}Ar and Rb-Sr ages, with evidence for heterochemical mica generations. We interpret them as a result of widespread hydrothermal circulation event(s). Tertiary overprint is generally absent, with the exception of a small area near Messina where biotite and muscovite underwent a complex recrystallisation history in the interval between 48 and 61 Ma.

Keywords Hercynian orogeny · Alpine overprint · Calabria-Peloritani massif · ^{39}Ar-^{40}Ar · U-Pb · Amphibole

S. De Gregorio (✉) · S. G. Rotolo
Dipartimento di Chimica e Fisica della Terra (CFTA),
Università di Palermo,
Via Archirafi, 36-90123 Palermo, Italy
e-mail: sofiadg@tiscalinet.it
Fax: +39-091-6168376

I. M. Villa
Isotopengeologie,
Erlachstrasse 9a, 3012 Bern, Switzerland

I. M. Villa
Dipartimento di Scienze Geologiche e Geotecnologie,
Università di Milano,
Bicocca, Italy

Introduction

The Peloritani Mts. represent the Sicilian portion of the Calabria-Peloritani metamorphic massif, which is a fragment of the Hercynian belt that has been thrust over the sedimentary units of the Apenninic domains during early Miocene (Amodio-Morelli et al. 1976). Hercynian metamorphism reached granulite grade in Calabria (Paglionico and Piccarreta 1978; Schenk 1980, 1984) and lower amphibolite grade in the Peloritanian sector (Ferla 1974). In late-Hercynian time the basement was widely intruded by granitoid bodies (Del Moro et al. 1982; Rottura et al. 1990). High pressure Tertiary metamorphism is present in northern Calabria, whereas in Aspromonte (Platt and Compagnoni 1990) and in the North-Peloritani (Messina et al. 1990) sectors the overprint is very variable or totally absent.

The Peloritani Mts. consist of a series of south-vergent crystalline nappes which are in contact with the underlying Apenninic-Maghrebian sedimentary units along the transpressive Longi-Taormina lineament (Bonardi et al. 1976). The metamorphic belt in the Peloritanian sector is imbricated in such a way to form an inverted metamorphic pile: the tectonically highest unit, the Aspromonte Unit, shows the highest metamorphic grade, and is overthrust on to the medium grade Mela Unit (Messina et al. 1997), which tectonically lies on the medium-low grade Mandanici Unit. The Mandanici Unit is in turn thrust over the lowest units: Fondachelli and Longi-

source: https://doi.org/10.7892/boris.89281 | downloaded: 1.8.2022

Taormina Units, which show a greenschist or even lower grade metamorphism.

The timing of the formation of the orogenic edifice is not well constrained. Unmetamorphosed to slightly metamorphosed Meso-Cenozoic cover sequences are sometimes interposed as very thin and dispersed tectonic slices between the Aspromonte and Mandanici Units (Atzori et al. 1975). This indicates at least a certain degree of post-Hercynian thrusting; however, the scarcity of age data hampers the understanding of the relative role played by (pre-) and post-Hercynian metamorphism and overprint. We decided to focus our attention on the Aspromonte and the Mela Units because they show well-preserved metamorphic peak and retrograde assemblages, respectively.

This work reports ^{39}Ar-^{40}Ar stepwise heating experiments on 11 amphibole, 9 biotite and 3 muscovite separates. Rb-Sr dating on biotite, muscovite and K-feldspar from one rock, and U-Pb stepwise leaching on one titanite were performed.

Previous geochronological studies

Much attention has recently been paid to the presence of a Tertiary overprinting event in the Peloritani Mts. Some papers focused on the meso-structural aspects (Cirrincione and Pezzino 1991, 1994), some on microstructural ones (Messina et al. 1990), and others integrated structural and petrological considerations with geochronological data (Bonardi et al. 1987; Atzori et al. 1994).

Existing radiometric data consist either of Rb-Sr whole-rock and/or mica ages, that is, an isotopic clock which is readily reset even by a weak hydrothermal episode (Krogh and Davis 1973), or on K-Ar whole-rock ages, i.e. a method rather unsuitable for polymetamorphic rocks (Geyh and Schleicher 1990, p. 62).

Age estimates for Hercynian basement paragneisses and augengneisses range from 262 to 292 Ma, and are considered cooling ages after the Hercynian metamorphism (Atzori et al. 1990). Post-tectonic peraluminous granitoids intruding the metamorphic basement (e.g. Capo Rasocolmo) have been dated at 293±9 Ma (Del Moro et al. 1982). Phengite ages obtained by Atzori et al. 1994, mostly on rocks belonging to the metasedimentary cover of the Mandanici Unit, range from 278 to 26 Ma and are interpreted as mixed ages due to the variable resetting of Hercynian micas during the Tertiary.

Zuppetta et al. 1984 analysed very low-grade metabasites from the structurally low Fondachelli Unit and reported a K/Ar whole-rock isochron at 217±3 Ma. According to these authors, this result should be interpreted as an age, which reflects the thermal disturbance related to the opening of a small oceanic basin, precursor of the Tethys opening.

Metamorphic conditions

We focused our attention and sampling on a SW–NE 30-km-long transect (Fig. 1) across the two tectonically highest units of the belt (Aspromonte and Mela Units; Fig. 2) which, on the basis of microstructural analysis, better show the superposition of metamorphic events.

The *Aspromonte Unit* (Ogniben 1960) is constituted mostly of paragneisses (Bt+Grt±Sil±St±Crd±Ky, where

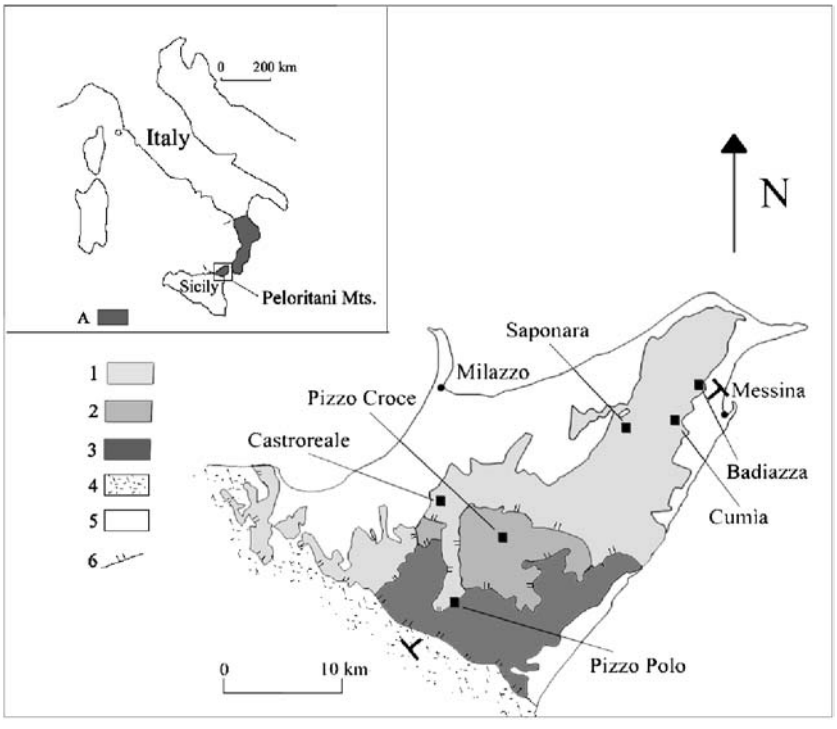

Fig. 1 Geological sketch map of the Peloritani Mts. *Inset* geographic location. *A* Metamorphic terrains of the Calabria-Peloritani massif. *1* Aspromonte Unit; *2* Mela Unit; *3* Mandanici Unit; *4* Fondachelli and Longi-Taormina Units; *5* Tertiary to recent deposits; *6* thrusts. Sampling areas are also shown

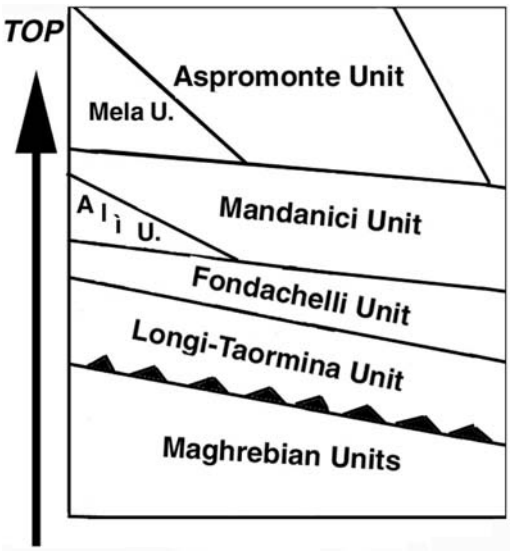

Fig. 2 Scheme of geometrical relationships in Peloritani Mts. (modified from Messina 1998a)

mineral abbreviations follow Kretz 1983), augengneisses (Kfs+Bt+Ms+Plg±Grt) and small bodies of amphibolites (Hbl±Grt±Ep±Cpx) and marbles (Cal±Cpx±Ms), all widely intruded by pegmatoid dikes. The total thickness is around 1,000 m. Hercynian metamorphism was in the range T=550–680 °C, P=0.3–0.5 GPa (Messina 1998b). The metamorphic field gradient is apparently increasing northwards, reaching conditions of anatexis in proximity of the northern coast of Sicily (Ferla 1972, 1974). The presence of a Tertiary overprint is reported near the city of Messina (Badiazza), where the overprint reached T $\leq$550 °C at P $\leq$0.45 GPa (Messina et al. 1990).

The *Mela Unit* (Messina et al. 1997) is constituted mostly of gneisses (grt±bt±and), micaschists (grt±bt±and) and amphibolites (hbl±grt±cpx) with a total thickness of around 700 m. This unit shows a peculiar metamorphic evolution characterised by a retrograde (Hercynian) metamorphism that affected an older high-pressure event (Borghi et al. 1995; Compagnoni et al. 1998). The metamorphic conditions of the Hercynian event were in the range T=500–550 °C, P=0.2–0.3 GPa (Messina et al. 1997). According to the latter authors, the emplacement of this unit in the metamorphic pile is of Alpine age.

Analytical techniques

All whole-rock samples (Table 1) were first analysed by XRF. Minerals were then analysed in polished sections, using an Oxford-Link SEM-EDS. Minerals were separated from the 0.06–0.12 mm and 0.12–0.25 mm grain size fractions using magnetic separator, heavy liquids and by hand-picking. Analytical protocols for ^{39}Ar-^{40}Ar, Rb-Sr and U-Pb analyses are described by Belluso et al. (2000), Pettke and Diamond (1997), and Frei et al. (1997), respectively. Results are presented in Tables 2, 3, and 4. Ar-Ar raw extraction data are reported in the appendix (Table 5). Results will be discussed in an order following their sampling area.

Interpretation of ^{39}Ar-^{40}Ar results is based on the general theory of multicomponent mixing (Villa 2001; Villa et al. 2000; Müller et al. 2002). Readers not familiar with its principles are referred to these papers for an in-depth discussion of the criteria allowing the identification of reservoirs, which would exceed the aim of this paper.

Table 1 Location of sampling sites

Sample	Locality	Subunit	Latitude[a], longitude[b]	Rock type	Association[c]
Mela Unit					
CRO 1	P. Croce		04′09″, 2°52′29″	Mafic amphibolite	Hbl, Plg, Chl
CRO 2	P. Croce		03′50″, °52′29″	Paragneiss	Qtz, Plg, Bt, Ilm
FR 1	T. Ferrà		04′00″, 2°51′43″	Amphibolite	Hbl, Cpx, Grt, Plg, Czo
FR 2	P. Croce		04′16″, 2°52′22″	Amphibolite	Hbl, Bt, Plg
FR 3	P. Croce		04′16″, 2°52′22″	Amphibolite	Hbl, Plg, Bt, Ilm
Aspromonte Unit					
VER 1	M. di Vernà	P. Polo	00′23″, 2°46′37″	Mylonitic augen-gneiss	Kfs, Qtz, Ms, Bt, Plg
CUM 1	Cumia	Cumia	10′18″, 3°03′13″	Amphibolite	Cum, Hbl, Kfs, Plg
CUM 3	Cumia	Cumia	10′28″, 3°03′05″	Amphibolite	Hbl, Plg, Chl
MAL 1	T. Malasà	Castroreale	05′32″, 2°46′13″	Epidote-amphibolite	Hbl, Plg, Czo
FLO 5	T. Cerasiera	Castroreale	04′36″, 2°50′45″	Mafic amphibolite	Hbl, Plg
BAD 1	V. Badiazza	Badiazza	02′49″, 3°03′27″	Gneiss	Ms, Bt, Grt, Plg
BAD 2	V. Badiazza	Badiazza	02′49″, 3°03′27″	Mylonitic gneiss	Bt, Ms, Grt, Plg, Kfs, Tur
PER 2	T. Peraredda	Saponara	10′45″, 2°59′53″	Amphibolic gneiss	Ath, Hbl, Grt, Cpx, Plg
PER 3	T. Peraredda	Saponara	10′45″, 2°59′53″	Mafic amphibolite	Hbl, Chl, Plg
PETR 1	T. Tiani	Saponara	11′18″, 2°59′55″	Pegmatite	Kfs, Bt, Ms, Qtz
STR 3	F. Stretto	Saponara	01′49″, 3°00′06″	Amphibolite	Hbl, Plg, Bt
STR 8	F. Stretto	Saponara	01′49″, 3°00′06″	Paragneiss	Bt, Plg, Qtz, Ms, Grt, And, Ilm, Tur

[a] Latitude 38°N
[b] Longitude referred to M. Mario (12°27′08″E of Greenwich)
[c] Mineral abbreviations from Kretz 1983

Table 2 Summary of $^{39}Ar/^{40}Ar$ data. Ar* is the radiogenic ^{40}Ar concentration (in nl/g) for a trapped atmospheric $^{40}Ar/^{36}Ar$ of 295.5. Concentration of K (‰). Cl (ppm) and Ca (%) were calculated from the reactor-produced ^{39}Ar, ^{38}Ar and ^{37}Ar, respectively

Sample	Mineral	Ar* (nl/g)	K (‰)	Ca (%)	Cl (ppm)	Assigned age (Ma)	Assignment criteria
Mela Unit							
CRO 1	Hbl	3.09	2.1	7.6	108	349±2	Ca/K>40
CRO 2	Bt	53.00	74.1	0.2	1474	Bt1: 239±2	Cl/K≤0.015
						Bt2: 187±2	Cl/K≥0.025
FR 1	Hbl	4.27	3.6	7.0	61	303±3	Ca/K=18–23
FR 2	Hbl	2.87	2.1	6.9	32	321±1	Ca/K=35
FR 3	Hbl	6.59	5.5	7.7	93	319±3	Ca/K>4
Aspromonte Unit							
Pizzo Polo subunit							
VER 1	Ms	83.82	92.0	0.4	81	301±2	Ca/K<0.05
Cumia subunit							
CUM 1	Hbl	6.37	1.4	6.4	206	607±13	Ca/Cl>500
CUM 3	Hbl	14.11	4.0	6.9	181	Am1: 523±2	Cl/K=0.031
						Am2: 888±3	Cl/K=0.048
CUM 3	Bt	31.44	65.0	0.8	180	156±1	Ca/K<0.13
Castroreale subunit							
MAL 1	Hbl	2.70	2.0	7.3	118	322±10	Ca/K=40
FLO 5	Hbl	2.19	1.3	6.8	60	–	–
Badiazza subunit							
BAD 1	Bt	11.64	65.6	0.1	2350	Bt1: >61	Cl/K<0.03
BAD 1	Ms	11.30	75.6	2.0	298	Bt2: <48	Cl/K>0.04
						≈50–60	Similar range
BAD 2	Bt	10.29	60.4	0.9	114	≈50–60	Similar range
Saponara subunit							
PER 2	Hbl	4.31	2.9	6.7	133	Am1: ≤330	Ca/K≤25
						Am2: ≥380	Ca/K≥27
PER 2	Bt	36.26	70.9	0.4	236	170±1	Ca/K≤0.11
PER 3	Hbl	2.88	1.7	7.7	33	Am1: 320±5	Ca/K<52
						Am2: 422±3	Ca/K>63
PER 3	Bt	30.14	58.7	1.4	92	164±2	Ca/K<0.10
PETR 1	Bt	30.54	73.6	0.2	275	142±2	Ca/K<0.02
PETR 1	Ms	51.05	82.7	0.1	61	207±2	Ca/K<0.015
STR 3	Hbl	5.32	3.9	6.9	107	Am1: 289±2	Ca/K=20
						Am2: 394±1	Ca/K=23
STR 3	Bt	15.77	46.0	4.1	232	96±2	Ca/K≤0.08
STR 8	Bt	31.84	70.6	0.2	75	150±1	Ca/Cl<15

Table 3 U–Pb data for titanite CUM 3. Pb ratios are corrected for blanks (80 pg total Pb) and for mass fractionation (1‰/amu). *Asterisks* denote radiogenic Pb isotopes. SumTit is the recalculated bulk mineral

	Total Pb (%)	$^{206}Pb/^{204}Pb$	1σ (%)	$^{207}Pb/^{204}Pb$	1σ (%)	$^{207}Pb^*/^{235}U$	1σ (%)	$^{206}Pb^*/^{238}U$	1σ (%)
Titanite Cum 3									
Leachate	70.4	18.772	0.07	15.695	0.07	6.9764	0.65	0.4611	0.65
Residue	29.6	23.703	0.30	16.125	0.30	0.5370	1.05	0.0472	1.05
SumTit						1.1737	0.55	0.0881	0.55

Table 4 Rb–Sr data for the pegmatite PETR 1. Two-point ages were calculated from ms-kfs and bt-kfs pairs, respectively

Sample	Min	Rb (ppm)	Sr (ppm)	$^{87}Rb/^{86}Sr$	$^{87}Sr/^{86}Sr$	2-Point age (Ma)	$^{87}Sr/^{86}Sr$ initial
PETR 1	Ms	253.7	51.1	14.44	0.751		
						208.8±1.6	0.7081
	Kfs	3.0	285.0	0.30	0.709		
						129.9±0.3	0.7084
	Bt	414.8	11.8	103.27	0.899		

Table 5 Ar–Ar stepwise heating results. All Ar concentrations are given in picolitres per gram (pL/g); errors are 1σ; Ar* denotes total ^{40}Ar minus atmospheric ^{40}Ar. The integrated values of K (wt‰) Ca (wt%) and Cl (ppm) were calculated from the total ^{39}Ar, ^{37}Ar and ^{38}Ar, the production ratios and the irradiation time. Ages are given in Ma

Step	T (°C)	^{40}Ar tot	^{39}Ar	^{38}Ar	^{37}Ar	^{36}Ar	Age±1σ
Mela Unit							
CRO 1 hbl (33.9 mg); J=2.842* 10–3; Ar*=3,090; K=2.1‰; Ca=7.6%; Cl=108 ppm							
1	717	248.10 ± 0.04	0.537 ± 0.007	0.888 ± 0.005	5.22 ± 0.07	0.532 ± 0.006	715.8
2	923	123.99 ± 0.02	1.311 ± 0.005	1.593 ± 0.011	21.32 ± 0.10	0.092 ± 0.005	352.6
3	981	415.31 ± 0.03	5.121 ± 0.008	1.506 ± 0.007	101.97 ± 0.30	0.138 ± 0.006	351.3
4	1,011	1,011.00 ± 0.11	13.343 ± 0.012	2.266 ± 0.007	268.35 ± 0.72	0.165 ± 0.006	347.1
5	1,041	559.96 ± 0.04	8.127 ± 0.010	0.728 ± 0.007	158.99 ± 0.48	0.099 ± 0.004	317.4
6	1,065	99.50 ± 0.04	1.216 ± 0.005	0.284 ± 0.006	24.03 ± 0.13	0.046 ± 0.005	340.6
7	1,108	180.16 ± 0.04	2.301 ± 0.007	0.479 ± 0.006	47.40 ± 0.19	0.046 ± 0.005	348.7
8	1,146	85.45 ± 0.04	0.986 ± 0.006	0.248 ± 0.007	20.13 ± 0.14	0.051 ± 0.004	344.4
9	1,280	482.20 ± 0.06	6.103 ± 0.009	1.393 ± 0.007	121.26 ± 0.36	0.104 ± 0.002	355.0
10	1,383	227.25 ± 0.04	3.065 ± 0.005	0.556 ± 0.006	53.51 ± 0.17	0.098 ± 0.005	313.6
CRO 2 bt (2.2 mg); J=2.845* 10–3; Ar*=53,000; K=74.1‰; Ca=0.2%; Cl=1.474 ppm							
1	539	5,156.30 ± 1.00	89.151 ± 0.095	11.832 ± 0.080	1.11 ± 0.26	5.87 ± 0.11	187.0
2	631	6,208.60 ± 1.80	119.14 ± 0.12	12.258 ± 0.105	1.01 ± 0.18	2.03 ± 0.12	226.9
3	710	10,236.40 ± 1.55	206.33 ± 0.21	17.750 ± 0.110	0.86 ± 0.23	0.87 ± 0.11	232.7
4	760	6,991.70 ± 0.80	141.11 ± 0.14	14.412 ± 0.090	0.87 ± 0.15	0.948 ± 0.080	229.0
5	832	4,870.25 ± 0.90	97.90 ± 0.13	11.362 ± 0.135	0.00 ± 0.00	0.21 ± 0.11	236.0
6	875	6,565.15 ± 1.00	132.58 ± 0.18	14.486 ± 0.075	0.37 ± 0.30	0.767 ± 0.060	230.1
7	917	8,636.35 ± 1.80	174.98 ± 0.19	18.618 ± 0.095	1.40 ± 0.17	1.001 ± 0.055	229.5
8	956	6,984.45 ± 1.55	138.59 ± 0.16	12.563 ± 0.085	2.14 ± 0.18	1.574 ± 0.090	226.7
9	1,015	4,012.09 ± 1.25	74.87 ± 0.080	5.428 ± 0.100	0.00 ± 0.00	0.97 ± 0.10	239.0
10	1,159	2,563.47 ± 1.15	41.71 ± 0.12	3.498 ± 0.085	2.95 ± 0.30	1.811 ± 0.090	233.9
11	1,396	1,791.60 ± 1.60	18.18 ± 0.10	2.540 ± 0.105	8.04 ± 0.23	3.301 ± 0.095	217.1
FR 1 hbl (16.5 mg); J=6.600* 10–3; Ar*=4,270 ; K=3.6‰; Ca=7.0%; Cl=61 ppm							
1	630	157.92 ± 0.02	1.143 ± 0.008	0.370 ± 0.015	1.31 ± 0.21	0.572 ± 0.010	−18.0
2	750	77.28 ± 0.02	0.486 ± 0.016	0.172 ± 0.013	1.04 ± 0.18	0.256 ± 0.007	78.2
3	910	269.89 ± 0.04	7.504 ± 0.016	3.265 ± 0.015	3.46 ± 0.30	0.342 ± 0.006	257.8
4	950	461.21 ± 0.08	14.795 ± 0.022	1.901 ± 0.010	7.78 ± 0.29	0.273 ± 0.011	292.4
5	980	1380.79 ± 0.13	47.998 ± 0.046	2.520 ± 0.014	22.30 ± 0.24	0.360 ± 0.013	299.6
6	1,000	490.93 ± 0.05	16.343 ± 0.022	0.822 ± 0.015	7.68 ± 0.30	0.215 ± 0.007	295.7
7	1,040	195.94 ± 0.05	5.755 ± 0.010	0.577 ± 0.017	5.05 ± 0.20	0.217 ± 0.013	269.6
8	1,080	335.99 ± 0.05	10.658 ± 0.016	0.875 ± 0.018	6.14 ± 0.29	0.208 ± 0.012	293.6
9	1,170	1,201.88 ± 0.13	40.268 ± 0.040	2.936 ± 0.013	24.21 ± 0.22	0.362 ± 0.008	308.6
10	1,380	657.61 ± 0.29	19.496 ± 0.022	1.392 ± 0.020	11.35 ± 0.18	0.474 ± 0.011	301.8
FR 2 hbl (30.4 mg); J=2.833* 10–3; Ar*=2,870; K=2.1‰; Ca=6.9%; Cl=32 ppm							
1	701	173.92 ± 0.03	1.000 ± 0.007	0.261 ± 0.003	4.39 ± 0.04	0.336 ± 0.006	348.4
2	911	110.41 ± 0.03	1.440 ± 0.006	0.155 ± 0.006	19.90 ± 0.10	0.127 ± 0.005	248.4
3	954	267.33 ± 0.03	3.404 ± 0.007	0.268 ± 0.008	67.92 ± 0.22	0.167 ± 0.004	311.2
4	973	378.70 ± 0.06	5.347 ± 0.011	0.400 ± 0.005	101.48 ± 0.34	0.045 ± 0.009	329.3
5	990	317.98 ± 0.03	4.557 ± 0.008	0.294 ± 0.008	81.97 ± 0.25	0.052 ± 0.006	320.4
6	1,009	100.96 ± 0.04	1.336 ± 0.006	0.103 ± 0.007	23.94 ± 0.12	0.030 ± 0.006	330.9
7	1,027	63.43 ± 0.04	0.769 ± 0.006	0.097 ± 0.005	14.67 ± 0.12	0.010 ± 0.004	372.8
8	1,063	174.06 ± 0.06	2.397 ± 0.005	0.174 ± 0.006	43.81 ± 0.14	0.038 ± 0.007	327.2
9	1,148	640.89 ± 6.58	8.958 ± 0.089	0.651 ± 0.007	156.76 ± 2.26	0.150 ± 0.002	321.0
10	1,282	729.93 ± 0.07	10.202 ± 0.011	0.743 ± 0.006	178.54 ± 0.50	0.171 ± 0.005	320.8
11	1,380	219.79 ± 0.08	2.853 ± 0.007	0.198 ± 0.006	48.82 ± 0.18	0.106 ± 0.004	318.4
FR 3 hbl (12.7 mg); J=6.600* 10–3; Ar*=6,590; K=5.5‰; Ca=7.7%; Cl=93 ppm							
1	710	1,032.36 ± 0.10	25.183 ± 0.031	3.079 ± 0.013	2.75 ± 1.13	1.715 ± 0.018	233.2
2	920	621.05 ± 0.06	25.062 ± 0.028	2.226 ± 0.019	9.85 ± 1.06	0.374 ± 0.007	229.1
3	955	464.27 ± 0.03	16.990 ± 0.026	1.831 ± 0.018	14.02 ± 0.82	0.268 ± 0.007	254.8
4	990	1,012.51 ± 0.10	33.664 ± 0.034	3.039 ± 0.017	48.60 ± 1.61	0.381 ± 0.009	299.2
5	1,020	2,719.57 ± 0.22	92.253 ± 0.087	6.261 ± 0.019	184.48 ± 0.92	0.596 ± 0.009	310.1
6	1,080	487.95 ± 0.06	15.589 ± 0.020	1.195 ± 0.013	41.70 ± 1.40	0.316 ± 0.013	290.0
7	1,170	1,036.41 ± 0.07	31.556 ± 0.031	3.246 ± 0.016	77.16 ± 1.73	0.530 ± 0.014	315.1
8	1,380	690.33 ± 0.04	15.260 ± 0.016	1.706 ± 0.016	33.42 ± 0.66	0.854 ± 0.006	322.2
Aspromonte Unit							
VER 1 ms (3.3 mg); J=2.938* 10–3; Ar*=83,820; K=92.0‰; Ca=0.4%; Cl=81 ppm							
1	607	2,977.42 ± 0.26	43.187 ± 0.091	2.12 ± 0.05	1.11 ± 0.08	2.406 ± 0.04	258.8
2	716	2,409.81 ± 0.33	52.901 ± 0.088	1.32 ± 0.07	1.69 ± 0.07	1.546 ± 0.07	185.6
3	741	18,508.73 ± 1.61	293.02 ± 0.27	4.52 ± 0.07	0.77 ± 0.18	1.841 ± 0.05	298.9
4	765	15,125.30 ± 2.27	241.52 ± 0.24	3.57 ± 0.06	0.40 ± 0.21	0.545 ± 0.04	301.8

Table 5 (continued)

Step	T (°C)	^{40}Ar tot		^{39}Ar		^{38}Ar		^{37}Ar		^{36}Ar		Age±1σ
5	791	6,112.88 ±	0.85	96.95 ±	0.12	1.55 ±	0.05	0.00 ±	0.00	0.317 ±	0.03	302.4
6	858	8,337.15 ±	1.58	132.92 ±	0.14	2.32 ±	0.09	1.12 ±	0.16	0.647 ±	0.08	298.8
7	945	13,229.15 ±	0.67	211.25 ±	0.20	3.18 ±	0.07	1.76 ±	0.30	0.864 ±	0.04	299.4
8	1,022	11,399.88 ±	0.76	180.87 ±	0.19	2.80 ±	0.06	2.18 ±	0.12	0.979 ±	0.05	299.4
9	1,159	6,747.39 ±	0.76	104.07 ±	0.11	1.63 ±	0.07	3.80 ±	0.19	1.073 ±	0.07	301.0
10	1,344	2,490.80 ±	0.67	33.047 ±	0.097	0.89 ±	0.05	23.73 ±	0.17	1.707 ±	0.04	293.9
CUM 1 hbl (26.8 mg); J=2.877* 10–3; Ar*=6,370; K=1.4‰; Ca=6.4% ; Cl=206 ppm												
1	713	2,425.22 ±	0.82	1.670 ±	0.011	2.203 ±	0.010	15.15 ±	0.11	5.401 ±	0.020	1609.2
2	921	2,216.89 ±	0.20	6.930 ±	0.013	7.978 ±	0.016	182.20 ±	0.58	1.077 ±	0.011	1068.8
3	960	712.22 ±	0.06	4.062 ±	0.009	1.837 ±	0.009	101.64 ±	0.34	0.453 ±	0.007	635.5
4	982	298.14 ±	0.07	1.363 ±	0.008	0.711 ±	0.010	36.99 ±	0.24	0.315 ±	0.006	666.4
5	1,000	154.23 ±	0.06	0.596 ±	0.006	0.336 ±	0.003	17.36 ±	0.19	0.202 ±	0.006	697.9
6	1,035	205.48 ±	0.07	0.798 ±	0.007	0.485 ±	0.007	21.33 ±	0.21	0.315 ±	0.006	630.8
7	1,089	337.99 ±	0.09	1.618 ±	0.005	0.867 ±	0.005	41.82 ±	0.17	0.294 ±	0.007	682.7
8	1,154	768.10 ±	0.14	3.177 ±	0.009	1.666 ±	0.010	85.33 ±	0.33	0.437 ±	0.005	842.7
9	1,287	914.01 ±	0.10	3.417 ±	0.009	1.860 ±	0.013	91.58 ±	0.35	0.522 ±	0.007	911.4
10	1,388	1,158.20 ±	0.49	4.387 ±	0.007	2.181 ±	0.011	108.91 ±	0.35	0.715 ±	0.007	889.2
CUM 3 hbl (31.3 mg); J=2.885* 10–3; Ar*=14,110; K=4.0‰; Ca=6.9%; Cl=181 ppm												
1	650	804.49 ±	0.02	0.795 ±	0.009	0.460 ±	0.007	3.86 ±	0.04	0.624 ±	0.005	2130.3
2	713	11,656.90 ±	0.58	2.268 ±	0.011	7.611 ±	0.021	5.48 ±	0.04	37.688 ±	0.131	917.6
3	924	10,831.76 ±	0.99	11.033 ±	0.013	8.927 ±	0.018	93.79 ±	0.27	30.899 ±	0.109	669.4
4	940	6,082.24 ±	0.54	14.942 ±	0.016	5.473 ±	0.013	142.38 ±	0.41	12.356 ±	0.045	700.6
5	962	2,153.98 ±	0.14	7.651 ±	0.008	1.982 ±	0.010	74.29 ±	0.21	3.580 ±	0.013	630.3
6	1,000	2,475.47 ±	0.38	10.124 ±	0.013	2.276 ±	0.008	96.16 ±	0.29	4.437 ±	0.017	522.6
7	1,037	1,499.52 ±	0.16	2.404 ±	0.009	1.151 ±	0.007	23.85 ±	0.11	4.019 ±	0.015	579.7
8	1,087	1,962.54 ±	0.20	4.494 ±	0.009	1.642 ±	0.006	48.52 ±	0.17	4.354 ±	0.017	657.1
9	1,152	1,812.44 ±	0.28	5.092 ±	0.010	1.549 ±	0.007	53.14 ±	0.17	2.377 ±	0.012	887.6
10	1,286	4,408.34 ±	0.42	17.519 ±	0.019	4.030 ±	0.009	178.14 ±	0.51	2.655 ±	0.011	851.4
11	1,388	1,082.09 ±	0.38	4.264 ±	0.010	0.987 ±	0.006	43.79 ±	0.15	0.967 ±	0.008	784.5
CUM3 bt (1.7 mg); J=2.894* 10–3; Ar*=31,440; K=65.0‰; Ca=0.8%; Cl=180 ppm												
1	541	2,919.97 ±	0.88	49.38 ±	0.11	3.16 ±	0.11	3.51 ±	0.42	5.63 ±	0.11	128.1
2	632	3,710.54 ±	1.24	86.00 ±	0.12	4.11 ±	0.14	1.63 ±	0.21	3.70 ±	0.12	152.3
3	711	7,037.18 ±	1.24	203.24 ±	0.21	6.71 ±	0.16	1.73 ±	0.22	2.33 ±	0.11	156.1
4	787	7,799.00 ±	0.88	222.25 ±	0.25	7.01 ±	0.10	8.30 ±	0.28	2.65 ±	0.12	157.7
5	858	3,600.74 ±	1.00	95.23 ±	0.18	2.94 ±	0.14	6.01 ±	0.34	2.24 ±	0.14	154.4
6	926	3,974.79 ±	0.94	96.85 ±	0.12	3.40 ±	0.21	8.20 ±	0.44	2.60 ±	0.11	165.1
7	1,002	5,348.01 ±	1.65	135.28 ±	0.17	3.98 ±	0.10	20.62 ±	0.16	2.589 ±	0.065	168.8
8	1,160	3,310.75 ±	0.71	73.31 ±	0.19	2.13 ±	0.11	9.27 ±	0.36	1.94 ±	0.12	185.2
9	1,397	1,945.19 ±	0.94	17.27 ±	0.14	0.51 ±	0.08	7.81 ±	0.37	4.082 ±	0.094	210.8
MAL 1 hbl (29.4 mg); J=2.852* 10–3; Ar*=2,700; K=2.0‰; Ca=7.3%; Cl=118 ppm												
1	714	416.54 ±	0.04	1.634 ±	0.006	0.910 ±	0.006	28.76 ±	0.14	1.192 ±	0.007	199.9
2	922	377.02 ±	0.04	4.937 ±	0.007	2.256 ±	0.006	102.14 ±	0.32	0.282 ±	0.005	293.3
3	962	295.40 ±	0.03	3.822 ±	0.008	1.019 ±	0.004	76.44 ±	0.26	0.173 ±	0.005	312.4
4	981	156.53 ±	0.04	2.032 ±	0.009	0.370 ±	0.005	37.98 ±	0.19	0.037 ±	0.006	345.5
5	999	73.69 ±	0.01	0.999 ±	0.009	0.202 ±	0.004	18.98 ±	0.17	0.086 ±	0.005	242.1
6	1,036	116.89 ±	0.02	1.562 ±	0.007	0.362 ±	0.007	31.01 ±	0.17	0.056 ±	0.007	313.9
7	1,069	203.50 ±	0.03	2.816 ±	0.008	0.636 ±	0.006	55.46 ±	0.21	0.082 ±	0.008	311.3
8	1,108	321.51 ±	0.05	4.292 ±	0.008	0.976 ±	0.004	85.40 ±	0.28	0.117 ±	0.004	325.3
9	1,149	346.03 ±	0.06	4.492 ±	0.009	1.091 ±	0.010	89.71 ±	0.29	0.111 ±	0.009	337.7
10	1,287	498.20 ±	0.05	6.387 ±	0.011	1.541 ±	0.009	128.03 ±	0.41	0.211 ±	0.005	331.4
11	1,388	612.87 ±	0.09	7.889 ±	0.011	1.725 ±	0.011	146.85 ±	0.43	0.278 ±	0.005	326.3
FLO 5 hbl (33.9 mg); J=2.825* 10–3; Ar*=2,190; K=1.3‰; Ca=6.8%; Cl=60 ppm												
1	710	506.39 ±		1.983 ±	0.005	0.816 ±	0.005	12.92 ±	0.05	1.222 ±	0.007	342.7
2	919	459.16 ±	0.06	3.841 ±	0.007	1.338 ±	0.006	85.18 ±	0.28	0.328 ±	0.007	438.7
3	979	650.95 ±	0.06	6.635 ±	0.009	1.324 ±	0.009	216.14 ±	0.65	0.341 ±	0.007	397.7
4	1,015	343.10 ±	0.04	3.612 ±	0.011	0.552 ±	0.009	133.17 ±	0.55	0.172 ±	0.006	391.6
5	1,042	145.52 ±	0.04	1.546 ±	0.009	0.263 ±	0.007	49.11 ±	0.30	0.111 ±	0.005	355.1
6	1,063	118.65 ±	0.05	1.161 ±	0.011	0.225 ±	0.008	37.03 ±	0.37	0.061 ±	0.005	413.6
7	1,107	136.20 ±	0.07	1.240 ±	0.010	0.227 ±	0.007	41.20 ±	0.34	0.090 ±	0.006	420.5
8	1,146	128.27 ±	0.08	1.129 ±	0.005	0.267 ±	0.009	37.01 ±	0.20	0.093 ±	0.008	424.0
9	1,281	283.20 ±	0.07	2.614 ±	0.008	0.517 ±	0.008	79.33 ±	0.33	0.192 ±	0.005	411.8
10	1,385	180.03 ±	0.07	1.617 ±	0.009	0.304 ±	0.004	42.85 ±	0.26	0.162 ±	0.004	389.6
BAD 1 bt (3.5 mg); J =2.905* 10–3; Ar*=11,640; K=65.6‰; Ca=0.1%; Cl=2,350 ppm												
1	546	2,364.93 ±	0.66	91.548 ±	0.097	17.652 ±	0.066	0.85 ±	0.09	5.114 ±	0.057	48.2
2	630	2,272.83 ±	0.91	147.37 ±	0.17	25.141 ±	0.086	0.87 ±	0.11	1.984 ±	0.057	59.0

Table 5 (continued)

Step	T (°C)	^{40}Ar tot		^{39}Ar		^{38}Ar		^{37}Ar		^{36}Ar		Age±1σ
3	712	1,371.69 ±	0.54	88.93 ±	0.10	14.675 ±	0.054	0.36 ±	0.11	1.111 ±	0.060	60.5
4	763	687.77 ±	0.40	41.004 ±	0.086	6.689 ±	0.043	0.29 ±	0.15	0.931 ±	0.054	52.0
5	834	951.21 ±	0.31	61.407 ±	0.071	10.171 ±	0.071	0.07 ±	0.10	0.828 ±	0.051	59.3
6	900	1,585.47 ±	0.54	117.22 ±	0.13	20.540 ±	0.077	1.21 ±	0.13	1.115 ±	0.063	55.3
7	970	3,988.86 ±	0.46	322.40 ±	0.29	54.68 ±	0.13	1.35 ±	0.15	1.672 ±	0.069	55.9
8	1,023	2,050.77 ±	0.66	156.52 ±	0.16	25.537 ±	0.091	0.95 ±	0.16	0.967 ±	0.040	58.2
9	1,094	580.93 ±	0.49	22.162 ±	0.054	3.601 ±	0.040	0.64 ±	0.18	1.072 ±	0.057	61.4
10	1,232	541.21 ±	0.37	3.915 ±	0.049	0.881 ±	0.051	1.90 ±	0.13	1.382 ±	0.049	169.7
11	1,395	918.59 ±	0.83	1.127 ±	0.051	0.587 ±	0.049	3.51 ±	0.20	3.036 ±	0.046	98.2
BAD 1 ms; (3.0 mg); J=2.909* 10–3; Ar*=11,300; K=75.6‰; Ca=2.0%; Cl=298 ppm												
1	597	2,334.35 ±	0.11	32.171 ±	0.053	3.800 ±	0.060	2.86 ±	0.18	7.293 ±	0.053	29.1
2	707	3,775.47 ±	2.53	176.54 ±	0.20	5.617 ±	0.087	1.81 ±	0.15	6.678 ±	0.047	52.8
3	760	5,731.17 ±	0.47	524.64 ±	0.47	9.618 ±	0.057	1.53 ±	0.17	2.796 ±	0.031	48.4
4	807	2,349.82 ±	0.37	185.20 ±	0.18	3.334 ±	0.060	1.76 ±	0.14	1.885 ±	0.077	50.1
5	841	1,192.13 ±	0.33	65.62 ±	0.11	1.411 ±	0.073	1.14 ±	0.22	1.739 ±	0.067	53.5
6	875	997.65 ±	0.57	35.167 ±	0.087	1.303 ±	0.087	3.21 ±	0.08	2.110 ±	0.053	55.0
7	937	916.81 ±	0.50	37.808 ±	0.047	1.004 ±	0.073	4.19 ±	0.15	2.312 ±	0.053	32.2
8	1,016	1,010.57 ±	0.47	51.63 ±	0.12	2.048 ±	0.073	9.49 ±	0.18	1.950 ±	0.047	43.7
9	1,153	1,286.87 ±	0.63	53.301 ±	0.087	5.429 ±	0.050	64.21 ±	0.22	2.395 ±	0.043	56.6
10	1,344	2,011.51 ±	1.13	33.758 ±	0.087	7.505 ±	0.053	81.45 ±	0.32	5.776 ±	0.067	47.8
BAD 2 bt (2.6 mg); J=2.901* 10–3; Ar*=10,290; K=60.4‰; Ca=0.9%; Cl=114 ppm												
1	551	2,873.63 ±	0.27	112.82 ±	0.13	4.395 ±	0.088	3.22 ±	0.16	6.173 ±	0.050	48.1
2	630	1,334.37 ±	0.77	94.69 ±	0.10	2.403 ±	0.100	2.19 ±	0.22	1.459 ±	0.062	49.2
3	711	1,751.10 ±	0.77	138.15 ±	0.14	2.228 ±	0.073	1.16 ±	0.15	0.920 ±	0.065	55.2
4	764	1,278.99 ±	0.46	92.73 ±	0.13	1.874 ±	0.096	0.85 ±	0.21	1.021 ±	0.054	54.3
5	830	1,643.13 ±	1.19	117.79 ±	0.17	2.253 ±	0.077	3.93 ±	0.14	1.137 ±	0.073	57.2
6	875	1,180.64 ±	0.46	66.840 ±	0.085	1.873 ±	0.062	3.73 ±	0.16	1.292 ±	0.054	61.5
7	917	1,334.63 ±	0.34	84.77 ±	0.11	1.891 ±	0.081	5.12 ±	0.17	1.199 ±	0.054	59.5
8	954	1,365.42 ±	0.54	81.34 ±	0.10	1.850 ±	0.104	11.35 ±	0.11	1.705 ±	0.065	54.7
9	1,010	1,411.89 ±	0.69	88.05 ±	0.12	1.779 ±	0.085	29.49 ±	0.19	1.281 ±	0.065	60.5
10	1,148	1,211.93 ±	0.65	61.427 ±	0.092	1.525 ±	0.085	14.90 ±	0.19	1.292 ±	0.069	69.5
11	1,283	656.82 ±	0.50	6.961 ±	0.077	0.211 ±	0.096	3.41 ±	0.12	2.024 ±	0.065	43.
PER 2 hbl (27.3 mg); J=2.865* 10–3; Ar*=4,310; K=2.9‰; Ca=6.7%; Cl=133 ppm												
1	715	429.26 ±	0.07	1.757 ±	0.011	0.69 ±	0.01	9.37 ±	0.07	0.933 ±	0.006	406.5
2	924	435.89 ±	0.10	5.087 ±	0.008	1.66 ±	0.01	50.52 ±	0.16	0.355 ±	0.005	313.5
3	962	737.97 ±	0.23	9.845 ±	0.011	1.98 ±	0.01	124.30 ±	0.36	0.181 ±	0.005	334.4
4	1,003	409.86 ±	0.04	5.584 ±	0.007	0.97 ±	0.01	68.72 ±	0.20	0.103 ±	0.011	327.3
5	1,028	126.35 ±	0.04	1.611 ±	0.005	0.33 ±	0.01	20.86 ±	0.09	0.049 ±	0.004	334.1
6	1,072	274.83 ±	0.10	3.309 ±	0.007	0.72 ±	0.01	46.39 ±	0.16	0.115 ±	0.005	349.3
7	1,113	463.28 ±	0.04	5.405 ±	0.010	1.16 ±	0.01	71.03 ±	0.22	0.121 ±	0.005	375.7
8	1,150	280.59 ±	0.07	3.366 ±	0.009	0.65 ±	0.01	44.19 ±	0.17	0.096 ±	0.004	357.8
9	1,280	1,520.88 ±	0.12	19.335 ±	0.021	3.73 ±	0.01	251.05 ±	0.72	0.304 ±	0.007	353.9
10	1,384	290.79 ±	0.05	3.579 ±	0.007	0.71 ±	0.01	44.43 ±	0.14	0.148 ±	0.005	332.2
PER 2 bt (1.8 mg); J=2.858* 10–3; Ar*=36,260; K=70.9‰; Ca=0.4%; Cl=236 ppm												
1	544	1,603.07 ±	0.89	30.031 ±	0.100	2.45 ±	0.09	0.53 ±	0.26	2.818 ±	0.078	127.7
2	637	2,928.10 ±	1.00	63.318 ±	0.128	2.89 ±	0.11	3.01 ±	0.32	2.553 ±	0.094	168.9
3	715	5,464.27 ±	1.39	149.942 ±	0.178	4.46 ±	0.10	0.40 ±	0.37	1.276 ±	0.078	167.0
4	791	6,419.56 ±	0.89	176.694 ±	0.189	3.59 ±	0.16	1.24 ±	0.23	0.755 ±	0.089	172.4
5	862	4,655.42 ±	1.06	118.469 ±	0.178	3.31 ±	0.13	0.72 ±	0.33	1.610 ±	0.106	173.4
6	920	6,229.28 ±	1.39	167.837 ±	0.172	5.31 ±	0.13	4.93 ±	0.34	2.145 ±	0.144	164.3
7	1,003	7,588.00 ±	1.11	206.997 ±	0.239	4.60 ±	0.08	11.62 ±	0.35	1.425 ±	0.083	170.3
8	1,161	5,238.32 ±	0.78	128.876 ±	0.144	3.39 ±	0.13	6.52 ±	0.41	2.091 ±	0.067	176.1
9	1,394	1,703.62 ±	1.28	11.467 ±	0.100	1.15 ±	0.08	6.21 ±	0.38	4.156 ±	0.078	202.4
PER 3 hbl (33.1 mg); J=2.872* 10–3; Ar*=2,880; K=1.7‰; Ca=7.7%; Cl=33 ppm												
1	707	434.79 ±	0.022	1.843 ±	0.006	0.402 ±	0.003	3.35 ±	0.02	0.722 ±	0.004	536.1
2	918	565.00 ±	0.045	4.824 ±	0.006	0.493 ±	0.005	59.51 ±	0.18	0.448 ±	0.006	420.3
3	957	418.89 ±	0.033	3.940 ±	0.005	0.389 ±	0.008	95.08 ±	0.29	0.168 ±	0.005	443.9
4	997	704.76 ±	0.069	8.709 ±	0.009	0.785 ±	0.010	260.09 ±	0.73	0.204 ±	0.005	363.9
5	1,022	277.89 ±	0.036	3.701 ±	0.007	0.305 ±	0.006	95.17 ±	0.31	0.096 ±	0.005	332.9
6	1,064	100.25 ±	0.019	1.109 ±	0.006	0.089 ±	0.007	28.26 ±	0.18	0.097 ±	0.004	320.5
7	1,106	135.57 ±	0.021	1.366 ±	0.010	0.133 ±	0.007	40.28 ±	0.31	0.101 ±	0.006	378.5
8	1,145	130.26 ±	0.039	1.310 ±	0.004	0.150 ±	0.008	39.00 ±	0.16	0.073 ±	0.005	402.0
9	1,220	178.76 ±	0.030	1.669 ±	0.007	0.180 ±	0.005	51.61 ±	0.25	0.110 ±	0.005	422.0
10	1,279	222.77 ±	0.042	2.192 ±	0.007	0.250 ±	0.007	66.59 ±	0.27	0.112 ±	0.006	417.6
11	1,384	329.51 ±	0.057	3.306 ±	0.007	0.382 ±	0.005	98.41 ±	0.32	0.180 ±	0.006	404.8

Table 5 (continued)

Step	T (°C)	^{40}Ar tot		^{39}Ar		^{38}Ar		^{37}Ar		^{36}Ar		Age±1σ
PER 3 bt (2.5 mg); J=2.868* 10–3; Ar*= 30,140; K=58.7‰; Ca=1.4%; Cl=92 ppm												
1	548	1,854.57	± 0.96	35.153	± 0.092	2.29	± 0.12	2.08	± 0.15	3.879	± 0.060	101.4
2	635	2,097.95	± 1.04	48.049	± 0.108	1.51	± 0.09	0.32	± 0.16	1.670	± 0.060	165.0
3	714	2,726.44	± 0.92	71.905	± 0.100	1.41	± 0.09	2.13	± 0.09	1.350	± 0.052	160.2
4	765	2,723.12	± 0.88	69.561	± 0.104	1.48	± 0.09	1.34	± 0.16	1.319	± 0.076	165.7
5	837	3,450.99	± 0.80	93.792	± 0.108	2.29	± 0.07	2.86	± 0.18	0.855	± 0.076	168.4
6	883	4,240.80	± 1.08	116.038	± 0.148	1.50	± 0.08	6.98	± 0.13	0.740	± 0.048	171.0
7	923	6,765.80	± 0.76	185.450	± 0.192	2.93	± 0.06	9.79	± 0.18	0.870	± 0.056	173.1
8	964	6,200.32	± 1.48	168.190	± 0.180	3.26	± 0.10	21.88	± 0.29	1.150	± 0.048	171.9
9	1,018	2,247.90	± 1.04	56.148	± 0.124	1.08	± 0.12	34.54	± 0.26	0.918	± 0.092	173.8
10	1,159	1,408.95	± 0.80	28.703	± 0.108	1.06	± 0.08	12.49	± 0.32	1.212	± 0.044	180.3
11	1,399	1,119.66	± 1.08	12.761	± 0.064	0.57	± 0.08	21.98	± 0.25	1.950	± 0.072	208.7
PETR 1 bt (3.6 mg); J=2.929* 10–3; Ar*=30,540; K=73.6‰; Ca=0.2%; Cl=275 ppm												
1	539	3,340.00	± 0.23	104.615	± 0.100	5.23	± 0.05	1.29	± 0.27	4.255	± 0.050	102.3
2	600	2,316.65	± 1.06	64.342	± 0.086	2.50	± 0.10	0.41	± 0.21	2.055	± 0.039	135.2
3	658	3,282.06	± 1.44	100.249	± 0.125	3.11	± 0.04	0.91	± 0.13	1.627	± 0.039	142.0
4	709	3,470.78	± 1.17	113.108	± 0.122	3.38	± 0.04	0.76	± 0.18	0.728	± 0.061	146.1
5	760	2,385.87	± 0.81	75.813	± 0.083	2.29	± 0.05	1.02	± 0.14	0.856	± 0.053	142.9
6	833	3,763.58	± 0.75	121.229	± 0.139	3.26	± 0.08	1.12	± 0.14	1.315	± 0.044	141.5
7	903	4,294.06	± 1.17	144.433	± 0.158	4.26	± 0.07	1.36	± 0.10	1.295	± 0.044	137.7
8	960	4,600.03	± 0.36	155.716	± 0.158	4.18	± 0.06	1.15	± 0.14	1.134	± 0.072	139.2
9	1,017	4,060.86	± 0.53	131.767	± 0.131	3.22	± 0.05	1.62	± 0.14	0.867	± 0.039	146.5
10	1,157	3,074.00	± 0.58	88.827	± 0.097	2.25	± 0.05	2.96	± 0.17	1.424	± 0.050	151.4
11	1,399	1,056.63	± 0.83	16.450	± 0.053	0.80	± 0.04	0.39	± 0.18	1.711	± 0.028	168.9
PETR 1 ms (2.4 mg); J=2.934* 10–3; Ar*=51,050; K=82.7‰; Ca=0.1%; Cl=61 ppm												
1	604	2,715.34	± 0.63	48.916	± 0.121	2.99	± 0.07	1.81	± 0.29	3.751	± 0.075	166.0
2	716	3,313.49	± 0.46	72.739	± 0.088	1.82	± 0.10	2.32	± 0.18	2.125	± 0.104	185.6
3	745	8,350.79	± 0.79	192.752	± 0.188	3.64	± 0.11	1.23	± 0.22	2.084	± 0.092	200.8
4	766	10,896.13	± 0.75	247.834	± 0.246	3.88	± 0.09	1.38	± 0.17	2.081	± 0.092	207.2
5	791	6,454.21	± 1.38	145.747	± 0.167	1.71	± 0.14	0.00	± 0.00	0.936	± 0.058	211.5
6	822	3,693.95	± 0.83	78.686	± 0.142	1.51	± 0.09	0.60	± 0.24	1.196	± 0.071	211.8
7	856	2,458.65	± 0.58	52.676	± 0.079	0.82	± 0.06	0.00	± 0.00	0.966	± 0.079	206.2
8	940	4,175.00	± 0.39	94.251	± 0.129	1.81	± 0.07	0.91	± 0.29	1.663	± 0.054	195.9
9	1,020	6,035.17	± 1.13	133.941	± 0.154	2.15	± 0.09	1.39	± 0.23	1.523	± 0.088	208.2
10	1,159	7,732.17	± 1.33	170.577	± 0.163	3.25	± 0.09	2.24	± 0.26	2.113	± 0.050	208.1
11	1,347	1,539.15	± 0.75	16.500	± 0.054	0.67	± 0.05	0.10	± 0.26	2.928	± 0.071	204.2
STR3 hbl (28.4 mg); J=2.914* 10–3; Ar*=5,320; K=3.9 ‰; Ca=6.9%; Cl=107 ppm												
1	716	764.49	± 0.13	7.996	± 0.012	1.045	± 0.006	14.80	± 0.05	1.055	± 0.007	276.4
2	922	804.67	± 0.04	12.439	± 0.012	2.865	± 0.006	98.39	± 0.28	0.407	± 0.009	272.3
3	962	1,571.93	± 0.11	21.576	± 0.020	2.947	± 0.010	245.88	± 0.69	0.320	± 0.006	334.3
4	982	668.74	± 0.06	9.965	± 0.012	0.925	± 0.010	105.91	± 0.31	0.136	± 0.005	310.0
5	999	288.61	± 0.03	4.391	± 0.007	0.395	± 0.004	43.70	± 0.14	0.108	± 0.008	288.9
6	1,036	238.23	± 0.05	3.249	± 0.009	0.333	± 0.009	35.30	± 0.14	0.113	± 0.005	310.0
7	1,089	300.00	± 0.04	3.763	± 0.008	0.443	± 0.005	43.04	± 0.15	0.113	± 0.007	344.8
8	1,154	359.29	± 0.06	3.858	± 0.011	0.473	± 0.011	44.77	± 0.17	0.145	± 0.007	393.0
9	1,283	468.74	± 0.04	5.146	± 0.007	0.604	± 0.005	57.55	± 0.17	0.148	± 0.005	395.3
10	1,383	607.79	± 0.05	6.959	± 0.007	0.725	± 0.011	74.69	± 0.21	0.190	± 0.006	380.7
STR 3 bt (3.5 mg); J=2.920* 10–3; Ar*=15,770; K=46.0‰; Ca=4.1%; Cl=232 ppm												
1	549	1,415.28	± 0.54	52.036	± 0.100	2.23	± 0.07	16943.1	± 467.9	2.062	± 0.051	251.6
2	635	1,449.15	± 0.54	62.431	± 0.077	2.03	± 0.05	2.79	± 0.16	1.126	± 0.071	91.9
3	714	3,392.83	± 0.37	165.170	± 0.160	4.07	± 0.04	6.29	± 0.17	0.838	± 0.063	97.7
4	764	2,864.71	± 0.66	132.835	± 0.177	3.69	± 0.04	26.68	± 0.13	0.752	± 0.063	102.1
5	834	1,686.70	± 0.69	70.210	± 0.097	2.34	± 0.07	40.59	± 0.17	0.971	± 0.040	102.4
6	883	1,072.04	± 0.37	36.794	± 0.063	1.44	± 0.04	22.87	± 0.18	1.218	± 0.049	99.6
7	925	1,326.40	± 0.51	45.423	± 0.083	1.63	± 0.06	45.13	± 0.27	0.905	± 0.054	119.4
8	963	1,702.49	± 0.54	53.097	± 0.080	2.13	± 0.06	91.52	± 0.34	0.954	± 0.037	136.6
9	1,022	1,302.57	± 0.54	42.360	± 0.074	1.36	± 0.06	35.28	± 0.23	0.819	± 0.060	127.8
10	1,160	1,298.27	± 0.71	29.439	± 0.040	1.18	± 0.07	35.35	± 0.15	1.640	± 0.034	140.7
11	1,396	1,212.35	± 0.74	10.425	± 0.043	0.93	± 0.08	23.63	± 0.16	3.099	± 0.049	145.1
STR 8 bt (3.4 mg); J=2.925* 10–3; Ar*=31,840; K=70.6 ‰; Ca=0.2%; Cl=75 ppm												
1	550	3,441.97	± 0.44	103.090	± 0.115	3.12	± 0.05	2.37	± 0.14	2.809	± 0.056	129.0
2	636	3,463.47	± 0.88	104.763	± 0.100	2.61	± 0.07	0.72	± 0.10	1.635	± 0.044	144.2
3	720	6,289.44	± 0.71	204.731	± 0.185	3.25	± 0.04	0.57	± 0.06	0.921	± 0.065	148.8
4	768	5,465.29	± 0.71	173.960	± 0.168	3.00	± 0.08	1.16	± 0.14	0.687	± 0.041	153.0
5	835	2,411.90	± 0.35	75.436	± 0.088	1.66	± 0.05	1.16	± 0.25	0.647	± 0.065	149.1

Table 5 (continued)

Step	T (°C)	^{40}Ar tot		^{39}Ar		^{38}Ar		^{37}Ar		^{36}Ar		Age±1σ
6	880	1,761.61	0.44	54.862	0.076	0.89	0.06	0.93	0.14	0.488	0.065	149.3
7	920	2,563.29	0.79	77.695	0.088	0.77	0.09	0.17	0.18	0.291	0.062	160.9
8	961	3,070.68	0.62	91.851	0.097	1.26	0.04	1.64	0.13	0.660	0.056	158.1
9	1,019	3,467.00	0.32	103.393	0.112	1.32	0.06	0.36	0.16	0.578	0.053	160.9
10	1,155	2,425.05	0.68	67.411	0.085	0.86	0.05	2.00	0.17	1.154	0.035	156.2
11	1,292	822.29	0.65	12.077	0.044	0.54	0.07	1.35	0.10	1.440	0.047	165.7

Results

Mela Unit

The studied amphibolites of the Mela Unit are characterised by a three-stage P–T-t evolution which instead has not been recorded in metarenitic samples (Rotolo and De Fazio 2001): (1) the first stage (regional metamorphism) is characterised by the growth of amphibole (Fe-hornblende to Fe-tschermakite) onto the main foliation. (2) The second stage (thermal peak, T≤630 °C, P≤0.5 GPa) is characterised by the post-tectonic growth of garnet±clinopyroxene±Ca-plagioclase. (3) The third stage (retrograde, T≤500 °C, P≤0.3 GPa) affected extensively the peak assemblages, substituting clinopyroxene by amphibole, garnet by actinolite + plagioclase coronas, and ilmenite by titanite (Fig. 3).

Petrographic evidence for post-metamorphic hydrothermal crystallisation, for both Mela and Aspromonte

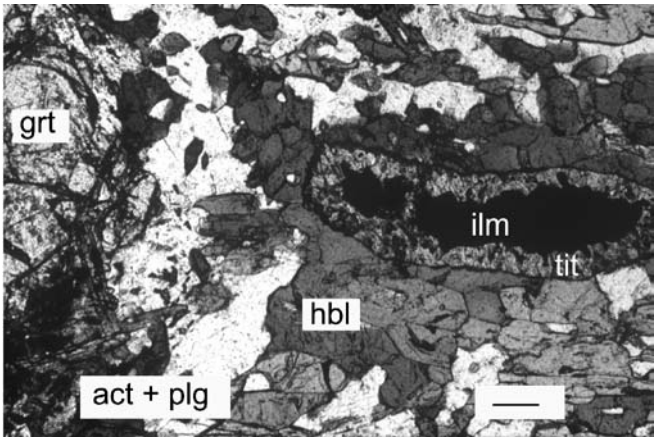

Fig. 3 Mela Unit: garnet amphibolite (sample FR1). Note the development of retrograde coronas of plagioclase+actinolite around garnet and of titanite around ilmenite. Plane-polarized light; *scale bar* 200 μm

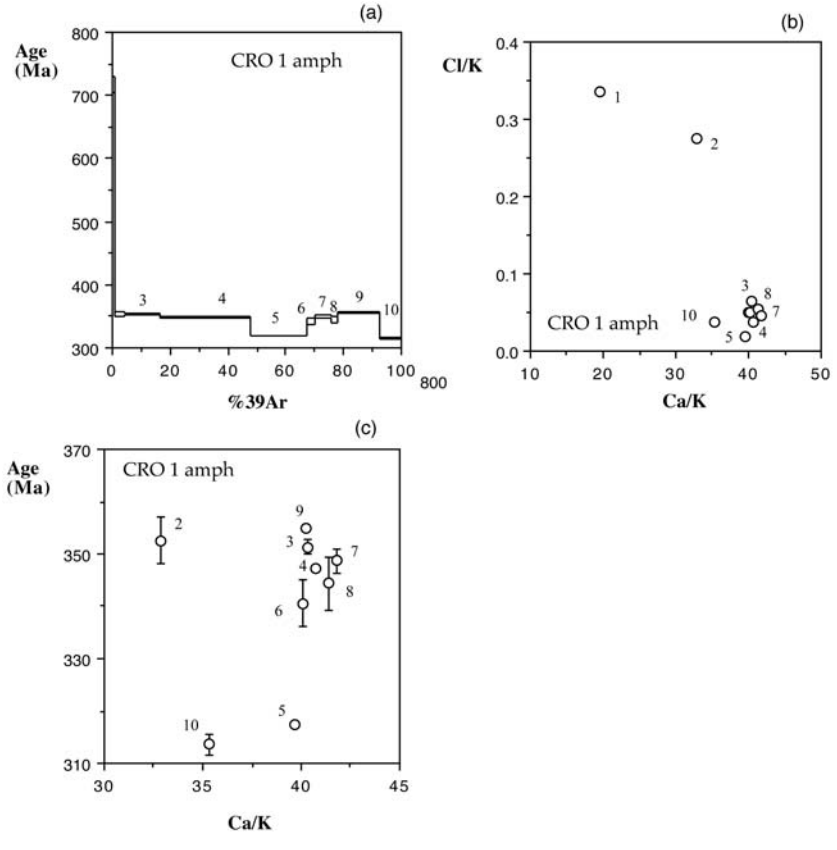

Fig. 4 **a** Age spectrum of amphibole CRO 1. *Numbers* identify the extraction steps (see appendix). **b** Chemical correlation diagram. Four *data points* (steps 1, 2, 5 and 10) deviate from the bulk of the amphibole (Ca/K≈41, Cl/K≈0.05) and are probably due to extraneous phases. **c** Ca/K age correlation diagram. The six *points* forming a cluster in (**b**) define an average age of 349±2 Ma

Units, is given by biotite cross-cutting foliation in amphibolites, post-tectonic tourmaline along shear planes, chlorite/epidote veins, calcite patches.

Sample CRO1: (mafic amphibolite). Hereafter the term *mafic amphibolite* will be used for rocks showing the most mafic compositions (i.e. MgO=14–19 wt%; Cr=700–1,400 ppm; Ni=350–700 ppm).

Amphibole composition ranges from hornblende to pargasite. Small veins of chlorite and epidote crosscut the foliation providing evidence for hydrothermal deposition.

The age spectrum (Fig. 4a) and the isochron give no immediately clear age information. In the compositional diagram (Fig. 4b), points show a wide scatter that rules out a binary mixing; following Villa (2001) such a scatter requires at least three or more Ar reservoirs. While amphibole sensu stricto is characterised by Ca/K>40 and ages of 349±2 Ma, there are steps (1, 2, 5, 10), with Ca/K<40, which do not pertain to amphibole but to extraneous phases and give younger ages around 315 Ma (Fig. 4c).

Sample CRO2: (paragneiss). CRO2 metarenitic gneiss is the host rock of the amphibolites. It is constituted of plagioclase (An20), quartz, and biotite. The latter occurs in two distinct generations: the first one marks the main foliation while the second one is post-tectonic and forms an angle of 45°–60° with the older one.

As expected, this sample does not give a plateau age (Fig. 5a): the spectrum is irregular because it reflects the mixture of the two biotite generations. We therefore use Cl/K as diagnostic ratio and plot the age as function of Cl/K (Fig. 5b). This allows us to define a trend between the two end-members, which are defined by (1) low Cl/K (0.015) and older ages (239±2 Ma), and (2) high Cl/K (0.025) and younger ages (187±2 Ma)

Sample FR1: (grt+cpx-bearing amphibolite). SEM-EDS microanalyses clearly show the presence of two different amphiboles in this rock, characterised (among others) by a different Ca/K ratio.

1. high-Al amphibole (Fe-tschermakite/Fe-hornblende), which crystallises along the main foliation, characterised by Al^{IV}=1.0–1.6 apfu, NaM4< 0.06 apfu, A-site filling=0.3–0.5 apfu. The Ca/K ratio is in the range 17–22.
2. low-Al amphibole (actinolite) in retrograde coronas around garnet. Its Ca/K ratio is much higher (200–270) than that of the Fe-tschermakite.

This sample gave an age spectrum in which six steps (containing 91% of the total ^{39}Ar) have ages around 300 Ma (Fig. 6a) and Ca/K ratios ranging from 18 to 23, identical to the Ca/K ratio (determined by SEM-EDS) of the Fe-tschermakite defining the main foliation.

In this sample, as in several other samples discussed below, it is seen that while individual steps can have uncertainties <1 Ma, the scatter between steps exceeds a few Ma and is thus statistically significant. This scatter does not closely correlate with Ca/K or Cl/K. It is possible that this scatter is an artefact due to differential recoil of the isotopes produced from Ca, Cl and K during irradiation (Onstott et al. 1995); this effect can become significant if the allochemical amphibole generations are intergrown on a scale <1 μm (Belluso et al. 2000). In this case, the age variations between steps have no real geological cause, and only reflect internal redistribution of the artificial Ar isotopes; the average of the pertinent steps, even if it appears to be statistically illegitimate, is thus probably least affected by recoil artefacts. As the statistical software we used for calculating the weighted averages (Ludwig 2000) has a built-in amplification factor that takes into account the deviations that exceed the purely analytical uncertainty, we feel safe in using the higher uncertainty associated with the weighted average because of the conservative way it is defined.

In this sample, the weighted average of the six steps mentioned above is 303±3 Ma, with a considerably higher uncertainty than that of individual steps (as low as 0.5 Ma).

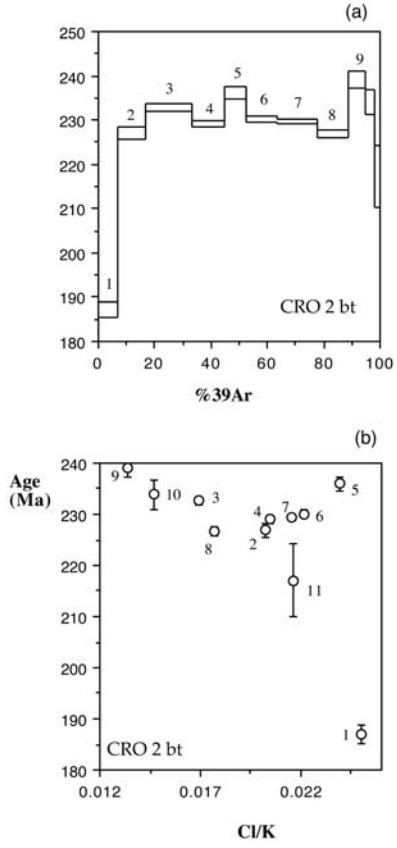

Fig. 5 **a** Age spectrum of biotite CRO 2. The irregularities reflect a mixture of at least two mineral generations. **b** Cl/K age correlation diagram. Two end members are identified: Cl/K=0.015 and age=239±2 Ma; Cl/K=0.025 and age=187±2 Ma

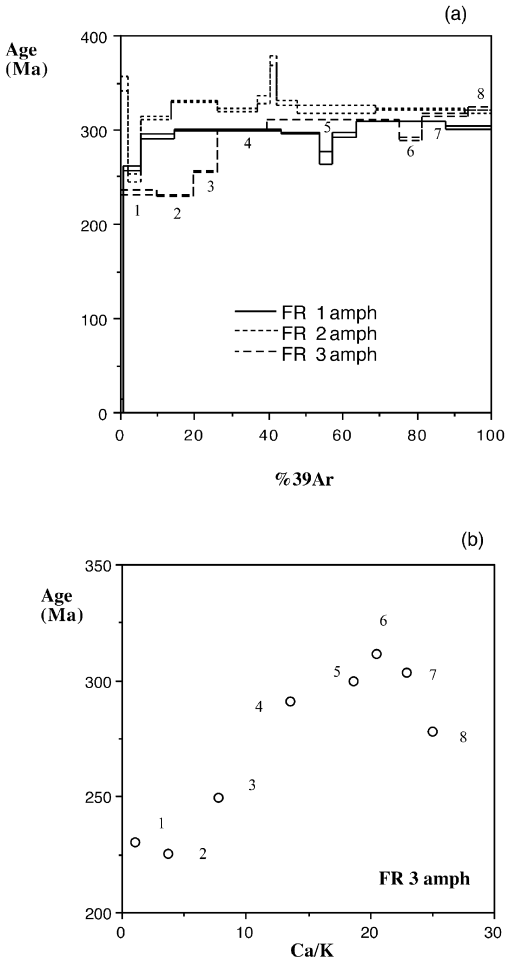

Fig. 6 **a** Age spectra of amphiboles FR1, FR2 and FR3 from amphibolites of the Mela Unit. **b** Ca/K age correlation diagram for amphibole *FR3*. The influence of a young, low-Ca mineral (presumably submicroscopic mica finely intergrown with amphibole) is clearly visible

Sample FR2 (bt-bearing amphibolite). This sample is constituted of a Mg-hornblende, plagioclase (An23) and sparse biotite flakes cutting across the foliation or forming small patches substituting amphibole.

In the age spectrum (Fig. 6a) the last three steps having a constant Ca/K ratio of 35±0.5 (not shown) and containing 52% of the total ^{39}Ar give an age of 320.6±0.6 Ma.

Sample FR3 (bt-bearing amphibolite). The amphibole is an edenitic hornblende characterised by a fine intergrowth of biotite plus amphibole. This is reflected in its Ar release patterns which show the contribution of two components (Fig. 6a, b):

– a mica (Ca/K<1) with an age around 230 Ma,
– an amphibole (Ca/K>4) with ages in the range of 315–322 Ma.

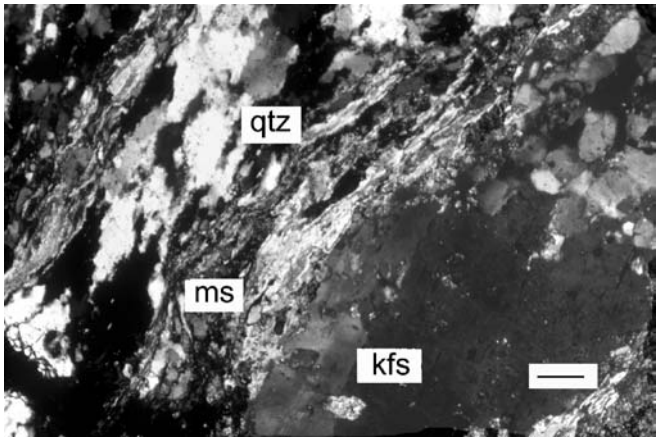

Fig. 7 Aspromonte "Unit" augengneiss VER1, sampled at the contact with the underlying Mandanici Unit. Note the mylonitic fabric. Crossed polars; *scale bar* 200 μm

The two components define a linear trend in Fig. 6b; the Ca-rich end-member has t ≈320 Ma, identical to the age of FR2.

Aspromonte Unit

Our observations show that the petrological and geochronological evolution of samples belonging to the Aspromonte Unit was very heterogeneous. Consequently, in the following discussion this unit will be split in different subunits on the basis of their regional location.

The characterising petrological features will be given separately for each subunit. Nevertheless, the common feature of all subunits, as regards the P–T-t evolution, is the absence of the retrograde metamorphism which pervasively affected the Mela Unit.

Pizzo polo subunit

Sample VER 1 (mylonitic augengneiss). This sample has been taken just above the tectonic contact between the Aspromonte Unit and the underlying Mandanici Unit. It is characterised by an evident mylonitic fabric, with quartz ribbons and strained muscovite anastomotic around K-feldspar porphyroclasts (Fig. 7). The Kfs+Ms+Qtz+Bt limiting assemblage allowed us to constrain the maximum pressure at 0.5 GPa (Si=3.14–3.20 apfu, following the calibration of Massonne and Schreyer 1987) at an inferred temperature of 550 °C, that is, shearing produced a complete recrystallisation at P≤0.5 GPa.

The age spectrum of VER 1 is fairly flat (Fig. 8), and, as expected for a single mineral generation, the Cl/K ratio is approximately constant. However, the dispersion of step ages exceeds their analytical errors (the dispersion parameter, MSWD, is >10). The ages of steps with low Ca/K ratios (i.e. most representative of a true mica) vary

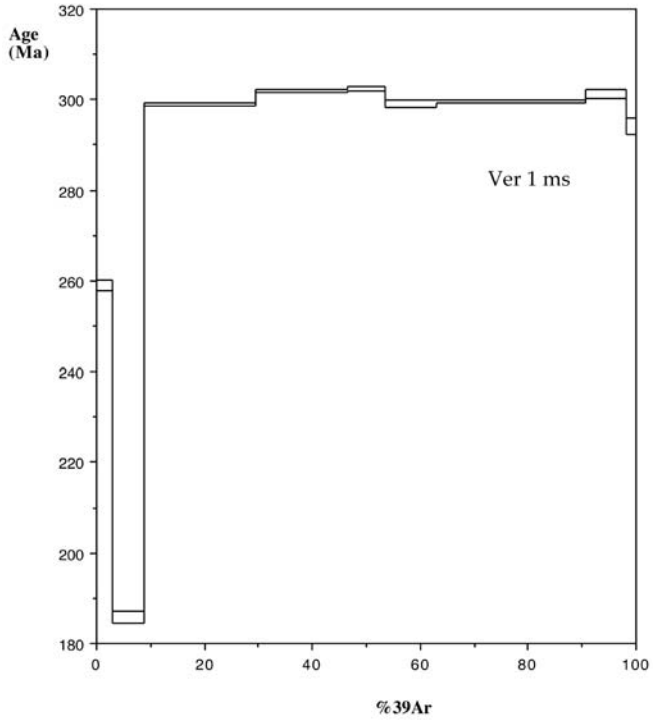

Fig. 8 Age spectrum of muscovite from mylonitic augen-gneiss VER 1, sampled at the tectonic contact between the Aspromonte Unit and the underlying Mandanici Unit. The age of mylonitization is 301±2 Ma

between 299 and 302 Ma. We therefore assign an age of 301±2 Ma to the mylonitization event.

Cumia subunit

The amphiboles from the Cumia area gave the oldest ages of the whole study (653–860 Ma); they show rather complex age spectra.

Sample CUM 1 (amphibolite). This sample shows a peculiar mineral assemblage: Mg-hornblende, cummingtonite, Ca-rich plagioclase (An 85–92), rutile and ilmenite. Plg-Hbl geothermometry failed to give reliable results, nevertheless, this assemblage suggests upper amphibolite facies conditions.

In the amphibole age spectra (Fig. 9a) the first two steps exceed 1 Ga; the other steps are in the range 650–950 Ma. Steps 1 and 2 characterised by Ca/K ratios no higher than the other steps (which have Ca/K=50–60) and high Cl/K; this suggests that they do not represent cummingtonite impurities, which would have extremely high Ca/K ratios, but rather admixture of a secondary phase.

The high ages raise the possibility that Ar excess (Ar_{xs}) could be present. By definition, an isochron is only legitimate if it is calculated on steps corresponding to cogenetic reservoirs. In this case, the presence of chemically heterogeneous reservoirs requires a careful selection. An example of a single reservoir is provided by the three steps with Ca/Cl>500, which account for 21.5% of the total gas and define a statistically acceptable isochron age of 607±13 Ma, with a trapped $^{40}Ar/^{36}Ar$ ratio of 368±25 and a dispersion parameter MSWD=0.05 (Fig. 9b). The high-temperature steps have lower Ca/Cl ratios and they might represent an even earlier amphibole generation, from which the 607-Ma amphibole grew. However, they do not define an acceptable isochron and the age of this supposed "amphibole generation 0" cannot reliably be estimated.

Sample CUM 3 (amphibolite). The principal difference with the CUM 1 sample is the much less calcic plagioclase (An 25–30), the absence of cummingtonite and ilmenite (titanite present). Amphibole composition ranges from edenite to pargasite. Small patches of calcite are rarely present along fractures.

The amphibole age spectrum (Fig. 9a) features step ages in the range 523–888 Ma, which define no isochron. The positive correlation between Cl/K and age (Fig. 9c) suggests a mixing between two different Ar reservoirs, whose end members are characterised by ages of 525 Ma (step 6) and 890 Ma (step 9).

The biotite data (Fig. 9d, e) show a fairly good negative correlation between Cl/K and age, and a positive one between Ca/K and age. Apart from step 1 (a minor Ca and Cl-rich secondary phase), steps 2–5 could be identified with the mica; their average is 156.5±1.3 Ma. High-temperature steps with a high Ca/K ratio suggest admixture of plagioclase impurities. Alteration appears to be of subordinate importance, as Cl concentrations are low; the total K concentration (6.5%) may be due to plagioclase intergrowth rather than simple alteration.

In this sample we also performed a U-Pb stepwise leaching experiment on titanite. The data are shown in Table 3 and Fig. 10a, b.

The $^{207}Pb/^{206}Pb$ age of 1.36±0.39 Ga (95% c.l.) obtained from leachate and residue (Fig. 10a) confirms the presence of a pre-Cambrian component, which can also be recognized from the concordia plot (Fig. 10b). The leachate and the residue define a discordia with intercepts at 142.5±4.3 Ma and 1,771±8 Ma. A cause of concern is the negative discordance of leach step Tit-1, which requires U loss. If the U loss (as uranyl complex) was caused by a hydrothermal circulation, both upper and lower concordia intercepts date a geological event. However, U-Pb fractionation could also be an artefact of the laboratory leaching (contrary to the gem-quality titanite studied by Frei et al. 1997). In any case, their sum corresponds by definition to the bulk sample; accordingly, the bulk point (which must lie on the discordia defined by leachate and residue) is shown in Fig. 10b. The model age of a single, discordant data point is underconstrained; however, it is limited by the lowest possible lower intercept, i.e. recent Pb loss, which results in an upper intercept age of 1,562±92 Ma. This age is the lower age limit for formation of the first generation of titanite in

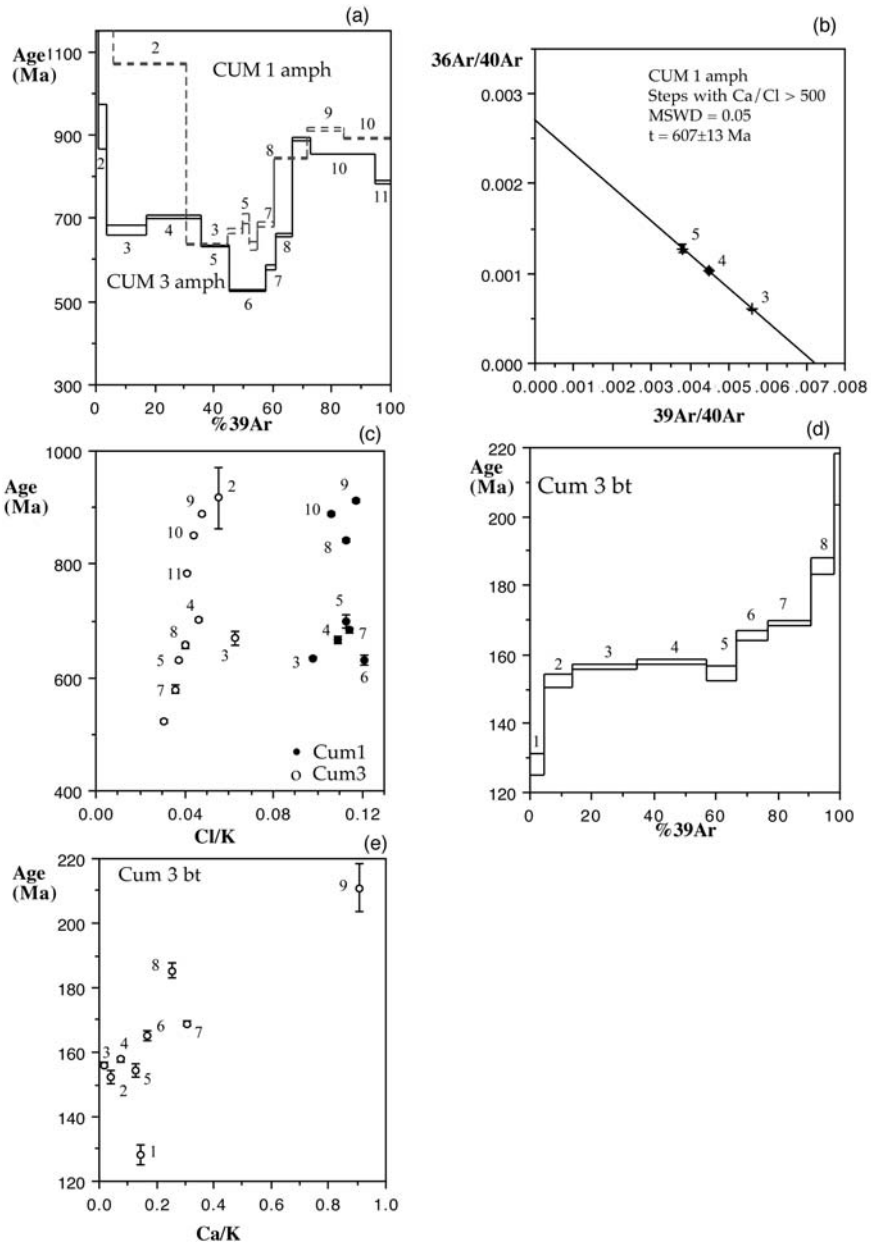

Fig. 9a–e Stepwise heating results of amphiboles from Cumìa Subunit. **a** Age spectrum of amphiboles CUM 1 and CUM 3. Both samples give Precambrian step ages. **b** Isochron diagram of amphibole CUM 1. Only points having a comparatively uniform chemical composition are likely to be cogenetic and can be regressed together; in this case, only steps 3, 4 and 5 (having Ca/Cl >500) fulfill this condition, and define a clear Precambrian isochron age of 607±13 Ma. This isochron indicates a lower age limit for the youngest among the different reservoirs of which CUM 1 is comprised. **c** Cl/K age correlation diagram. Sample CUM 1 does not define a clear linear trend, i.e. it requires a mixture of at least three components; as the uncertainties on the Cl/K values are smaller than the symbols, it is not legitimate to calculate an average Cl/K as if the sample were monomineralic and isochemical. On the contrary, CUM 3 appears to mainly be a binary mixture between two reservoirs having ages of $\leq$ 525 and $\geq$890 Ma. **d** Age spectrum of biotite CUM 3. **e** Ca/K age correlation diagram for biotite CUM 3. Only the steps with the lowest Ca/K ratios represent true biotite; they give an average age of 156.5±1.3 Ma

CUM 3. The Proterozoic age (1.77 or 1.56 Ga) supplements very well the Late Proterozoic amphibole ages and indicates a remarkable antiquity for the protolith of the Cumia Subunit. In our preferred interpretation, the lower intercept age dates a hydrothermal circulation (at 142 Ma, an age found in most micas of the study area); a recent laboratory fractionation cannot be ruled out, but this has little influence on the interpretation of the Proterozoic formation age.

Castroreale subunit

Sample MAL 1: (epidote-bearing amphibolite). Small pockets of plagioclase+epidote+titanite rim the main foliation amphibole. The latter presents a wide substitutional trend from hornblende towards pargasite, demonstrating a clear chemical heterogeneity. Temperature estimates (plg-hbl geothermometry, Holland and Blundy 1994) are in the range 530–620 °C. Low pressure of crystallisation is suggested by low NaM4 in amphiboles (<0.005 apfu).

The age spectrum (Fig. 11a) is discordant but the chemical (Fig. 11b) and Ca/K age (Fig. 11c) correlation diagrams show one cluster of points with Ca/K=39.9–40.6, Cl/K=0.049–0.058, and t=311–337 Ma (and an average age of 322 Ma); this cluster is interpreted as a slightly zoned amphibole. In addition, extraneous phases with both higher and lower Ca/K and Cl/K are inferred from the correlation diagrams (Fig. 11a, b); this points to a complex history of heterogeneous recrystallisation in

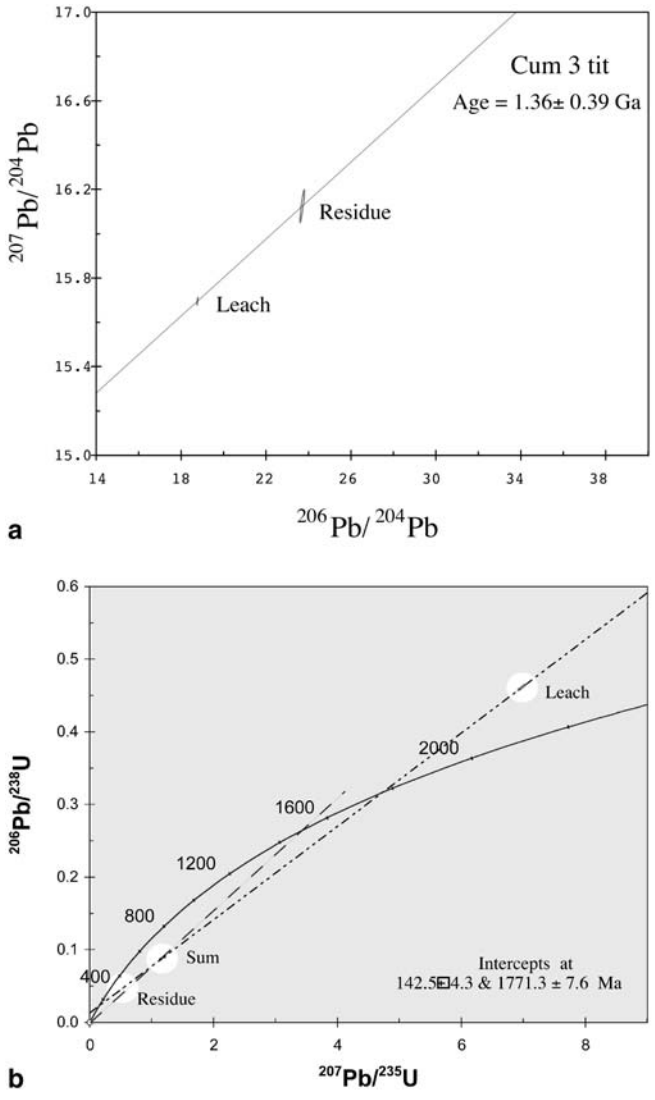

Fig. 10a, b Pb-Pb and U-Pb stepwise leaching results on titanite CUM 3. **a** $^{207}Pb/^{206}Pb$ isochron diagram. Leachate and residue define an age of 1.36±0.39 Ga (95% confidence level). The $^{207}Pb/^{206}Pb$ age is not affected by possible (but unlikely) fractionation of U and Pb during stepwise leaching, and is therefore conclusive proof that metamorphic titanite grew during the Mesopreoterozoic. **b** Concordia diagram. Leachate and residue define a discordia with intercepts 142.5±4.3 and 1,771±8 Ma (*dot-dashed line*). Even if there had been a laboratory fractionation of U from Pb, the reconstituted bulk titanite point (labelled as Sum Tit) defines a minimum upper-intercept age of 1,562±92 Ma

this sample.

Sample FLO5 (mafic amphibolite). This sample is almost entirely constituted of amphibole (Mg-hornblende) with scarce amount of plagioclase. Plagioclase-hornblende geothermometry (Holland and Blundy 1994) gave values of 570±40 °C.

The amphibole age spectrum (Fig. 11a) gives ages between 355 and 450 Ma; the Cl/K-Ca/K correlation (not shown) does not indicate a simple binary system but rather a complex mixture. The correlation diagrams show only a vague positive correlation between Cl/K ratios and age, but no clear age assignment. Calculating an isochron is not legitimate in the case of a multicomponent mixture, as indeed shown by the MSWD value of 34 obtained by regressing steps 3–9.

Amphibole ages are not constant in this Sub-Unit. Given the large number of reservoirs required by the Ar data, it is possible that one or more pre-Hercynian (Devonian, maybe older?) amphibole relics are preserved to different extents in the different samples; it is also possible that the Castroreale Sub-Unit will be shown by more detailed investigation to be itself heterogeneous.

Badiazza subunit

Samples from this area are characterised by shear fabric structures, and various stages of mineral growth (particularly garnet) after the regional Hercynian metamorphism (see Messina et al. 1990 for a detailed description). Post-tectonic tourmaline crystallises along shear planes.

Biotite and muscovite have indistinguishable ages around 50–60 Ma. This suggests a discrete period of pervasive shear recrystallisation limited to this area.

Sample BAD 1 (bt+ms+grt gneiss). Both muscovite and biotite have K concentrations well below stoichiometry (7.6 and 6.6%, respectively), indicating substantial degradation. Accordingly, both age spectra are discordant, with step ages younger than 61 Ma (Fig. 12a). The muscovite shows no correlation between Cl/K and age (Fig. 12b); the four steps with the lowest Cl/K ratios have scattered ages. In contrast, biotite (filled circles in Fig. 12b) does show a negative correlation, suggesting a mixing between two reservoirs: a young, Cl-rich one with t <48 Ma and Cl/K >0.04 (denoted as A in Fig. 12b), and one with Cl/K <0.03 and t >61 Ma (B in Fig. 12b). Steps 9, 10 and 11 (collectively containing 2.6% of the total Ar) have increasing Ca/K ratios due to calcium-rich impurities.

Sample BAD 2: (bt+ms+grt+tur mylonitic gneiss). The biotite age spectrum overlaps the BAD 1 biotite spectrum (Fig. 12a). Its Cl concentration is extremely low for a biotite; there is no clear correlation between Cl/K and age (Fig. 12b). A very low K concentration (K=6.0%) and high Ca/K ratios suggest that impurities and/or alteration products are more abundant in this sample.

Saponara subunit

Sample PER 2 (amphibolic gneiss). This granoblastic rock shows a rather faint foliation, marked by plagioclase (An 40), quartz, Fe-tschermakitic hornblende and subordinate amounts of Fe-anthophyllite; garnet is post-tectonic and unzoned (alm69, gro19, pyr10, sps2). Small amounts of clinopyroxene, substituting amphibole, are present. Bi-

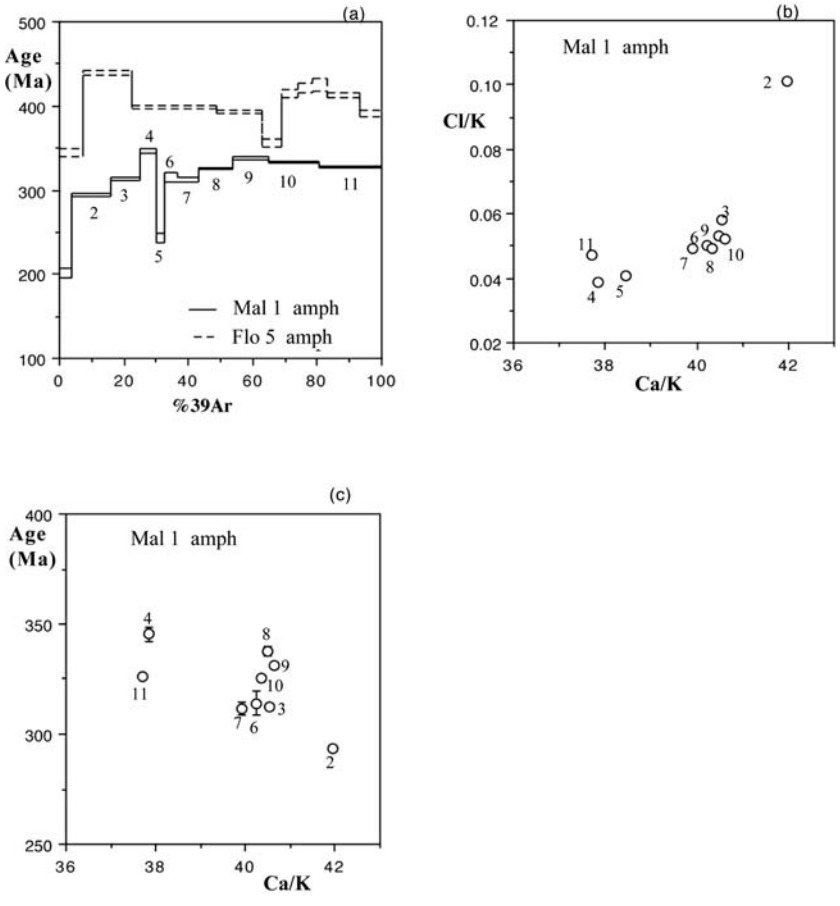

Fig. 11a–c Stepwise heating results of amphiboles from amphibolites of the Castroreale Subunit. **a** Age spectrum of amphiboles MAL 1 and FLO 5. **b** Chemical correlation and **c** Ca/K age correlation for MAL 1 amphibole; both suggest a mainly binary mixing trend. The cluster of points having Ca/K=39.9–40.6, Cl/K=0.049–0.058, and t=311–337 Ma are identified as amphibole

otite is present in rare post-tectonic flakes cutting across the foliation.

Geothermometry gave values in the range 640 °C (Plg-Hbl, Holland and Blundy 1994), 590 °C (Grt-Hbl, Graham and Powell 1984), in good agreement with the very narrow stability field of antophyllite (620–660 °C at 0.5 GPa, Winter 2001).

In the amphibole age spectrum (Fig. 13a), 90% of the released ^{39}Ar corresponds to amphibole having Ca/Cl >570. These steps gave ages in the range 327–376 Ma and define no isochron with an acceptable scatter. The positive correlation of age with Cl/K (Fig. 13b) and Ca/K (Fig. 13c) identifies one "young" amphibole generation, slightly younger than 330 Ma, and one (or, more probably, two) older ones, the oldest amphibole being $\geq$380 Ma.

The biotite appears not to be pervasively altered on account of its K concentration of 7.1%. Its age spectrum gave an average age of 170±1 Ma (Fig. 13d).

Sample PER 3 (mafic amphibolite). This rock is constituted almost totally by amphibole (Mg-hornblende) and apatite (ca. 3 vol%). Plagioclase (An 53) and biotite are rare, the latter being present in post-tectonic flakes cutting across the foliation. Plg-Hbl geothermometry (Holland and Blundy 1994) gave values around 640 °C.

The Mg-hornblende age spectrum gives ages in the range 330–430 Ma (Fig. 13a). The correlation diagrams (Fig. 13b, c) suggest a mixing between two end-members (A and B in Fig. 13b, c) characterised by ages of 422±3 Ma and 320±5 Ma, respectively. The ages of these end-member amphiboles are in excellent agreement with those inferred from PER 2.

The biotite step ages (Fig. 13d) are mostly in the range 160–170 Ma. The K concentration, 5.9%, is markedly lower than that of PER 2 and points to a more extensive alteration. The steps with Ca/K<0.1 are those most likely to reflect true mica with least contamination from extraneous phases; they average 164±2 Ma, significantly lower than the less altered mica PER 2.

Sample PETR 1 (pegmatite). This medium grained unfoliated pegmatite (Kfs+Ms+Bt+Qtz) cuts across the foliation of the hosting gneiss reflecting thus a post-metamorphic event. Rb/Sr isochrons were obtained for the pairs Kfs-muscovite and Kfs-biotite (Table 4) and gave ages of 209±1.6 and 130±.3 Ma, respectively.

The muscovite age spectrum is discordant (Fig. 14a); steps 3–11 have Ca/K<0.03 and Cl/K<0.0012. These steps presumably contain only minor amounts of alteration phases; their ages range between 196 and 212 Ma. Correlation diagrams (Fig. 14b) do not allow a close identification of reservoirs. As the K concentration, 8.3%,

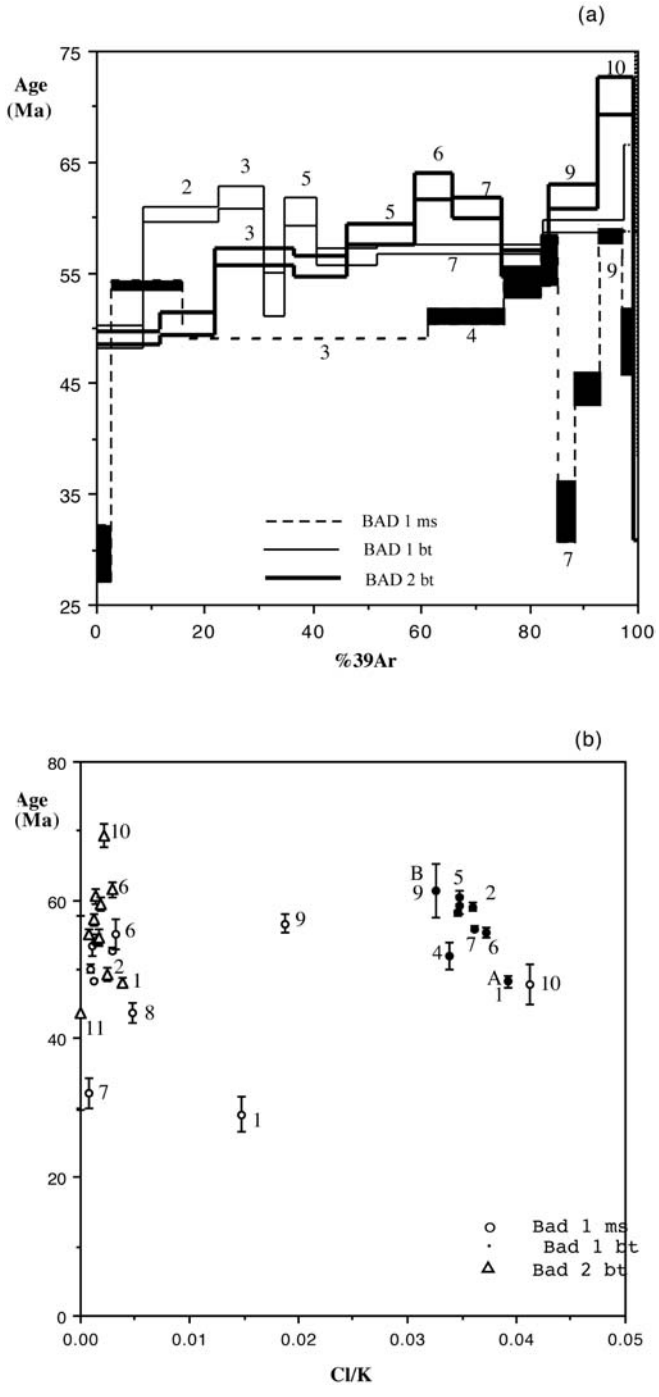

Fig. 12a, b Stepwise heating results of samples from Badiazza Subunit. **a** Age spectra of BAD 1 muscovite and biotite, and BAD 2 biotite. All step ages lie in the range 40–65 Ma; the age spectra are irregular because all reflect a mixture of more than one mica generations. **b** Cl/K age correlation diagram. Biotite BAD 1 defines a linear trend, indicative of a binary mixing. Criteria for the diagnosis, the identification, and the age assignments are discussed in the text, in Villa et al. (2000) and in Villa (2001). In the binary mixing of biotite BAD 1 one reservoir has an estimated age of 48±1 Ma and a Cl/K ratio of 0.04 while the other reservoir is slightly older and Cl-poorer (t=61±1 Ma, Cl/K=0.03). In contrast, muscovite BAD 1 and biotite BAD 2 do not show a simple binary mixing; the several (three or more) reservoirs of which these two samples consist confirm the age range between ca. 30 and ca. 70 Ma but defy a simple deconvolution

is nearly stoichiometric, we presume that the muscovite is unaltered, and we assign it a weighted average age of 207±2 Ma. We also note that the integrated age (which is the only part of a ^{39}Ar-^{40}Ar dataset that can be compared with a Rb-Sr bulk mineral age) is 203±1 Ma, identical to the Rb-Sr age.

The biotite data also indicate a mixture between two components (Fig. 14 c): (1) an alteration phase with Cl/K=0.007 and an age of 102±1 Ma, (2) the second with Cl/K=0.002, Ca/K=0.02 and an age of 142±2 Ma. The integrated age is 139±1 Ma and is again identical to the Rb-Sr age.

The identity of Rb-Sr and ^{39}Ar-^{40}Ar ages is strong evidence that these ages date crystallisation at low temperature, presumably in a hydrothermal event, because in conventional thermochronology the "closure temperatures" for Rb-Sr and K-Ar are assumed to be very different.

Sample STR 3 (amphibolite). Amphibole shows a wide substitutional trend from hornblende to pargasite. Biotite flakes cut across the foliation or form small patches substituting amphibole. Plg-Hbl geothermometry (Holland and Blundy 1994) gave values in the range 615–650 °C.

The amphibole age spectrum (Fig. 15a) is characterised by: (1) a secondary (micaceous?) component, released at T <900 °C, with Ca/K<4 and an age of 276±1 Ma, and (2), a mixture between two Ar reservoirs released at higher temperatures, the first having Ca/K=20 and an age of 289±2 Ma, the second one with Ca/K=23 and an age of 394±1 Ma.

The biotite has a non-stoichiometric K concentration (4.6%); this may be due to abundant Ca-rich impurities intergrowth at a very fine scale, as suggested by the high Ca concentration (4.1%). Its age spectrum (Fig. 15a) shows the effect of mixing two components: (1) a mica with Ca/K<0.08 and an age of 96±2 Ma, (2) a calcic contaminant with Ca/K>4.5 and an age >145 Ma (Fig. 15b).

Sample STR 8 (ms+bt+grt+ and +tur paragneiss). Biotite is present either in fine flakes along the foliation or in larger size crystal clots. Large andalusite poikiloblasts are clearly post-tectonic; garnet and muscovite are rare. Grt-bt geothermometry (Ferry and Spear 1978; Indares and Martignole 1985) is in the range 430–490 °C. Post-tectonic tourmaline occurs in biotite clots.

The biotite has a K concentration of 7.1% (Table 2) and gave a discordant age spectrum (Fig. 15a). It shows a complex mixing pattern: a Cl-rich alteration phase with an age of 129±1 Ma, a "true mica" with Ca/Cl<15 and an age of 150±2 Ma, and a contaminant with Ca/Cl>50 and an age >160 Ma.

In summary, two Saponara amphiboles have yielded Devonian ages. This sets this sub-unit apart from other terrane slivers that record younger Hercynian ages, and from the Cumia cummingtonite amphibolite subunit, which has clear Precambrian relics.

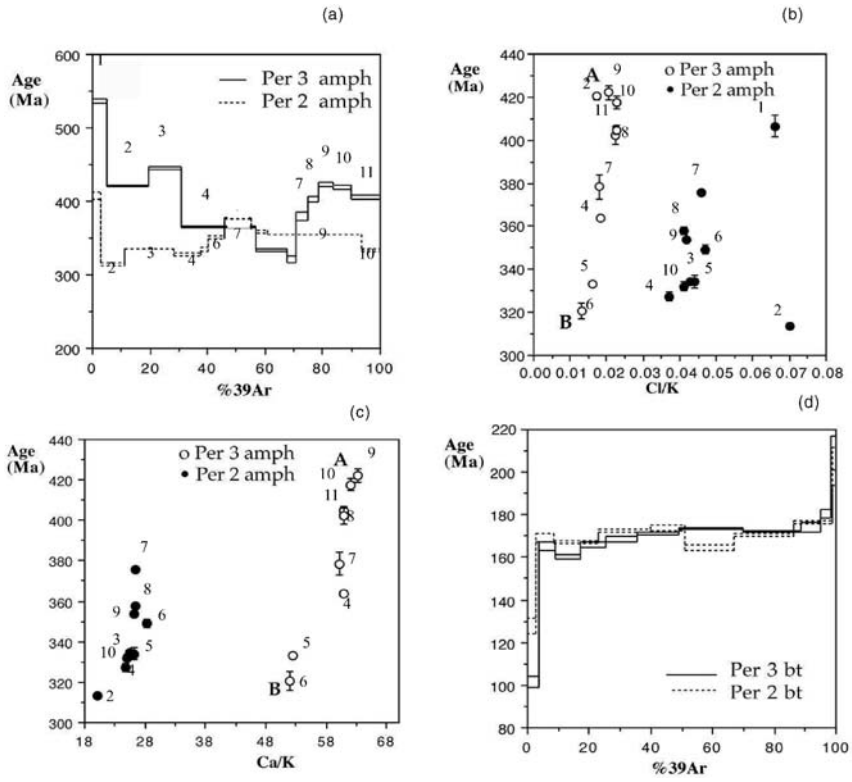

Fig. 13a–d Results for amphiboles and biotites from amphibole gneiss PER 2 and mafic amphibolite PER 3 (Saponara Subunit). **a** Amphibole age spectra. **b** Cl/K age correlation diagram. The fairly good linear trends indicate that most of the ^{40}Ar is contributed by just two reservoirs. For sample PER 3, letters *A* and *B* identify steps that approach the end-member compositions; their ages are estimated as 425 and 320 Ma, respectively. **c** Ca/K age correlation diagram. The amphibole reservoirs *A* and *B* are the same as those in Fig. 13b. **d** Biotite age spectra

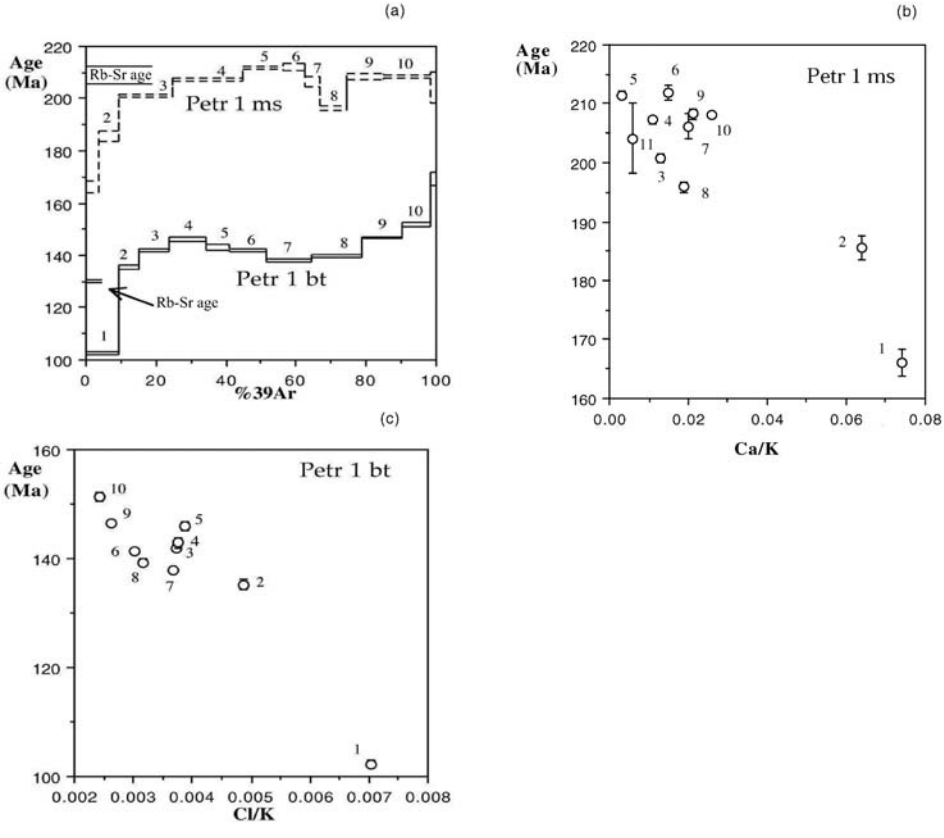

Fig. 14a–c Results for pegmatite PETR 1 (Saponara Subunit). **a** Age spectra of muscovite and biotite. The Rb-Sr bulk mica ages (Table 4) are shown near the ordinate axis; they are indistinguishable from the bulk K-Ar ages calculated from the sum of all steps. **b** Ca/K age correlation diagram for muscovite. Pure mica is Ca-free and has an age of 206±3 Ma. **c** Cl/K age correlation diagram for biotite. A high-Cl alteration phase is responsible for step ages as low as 100 Ma

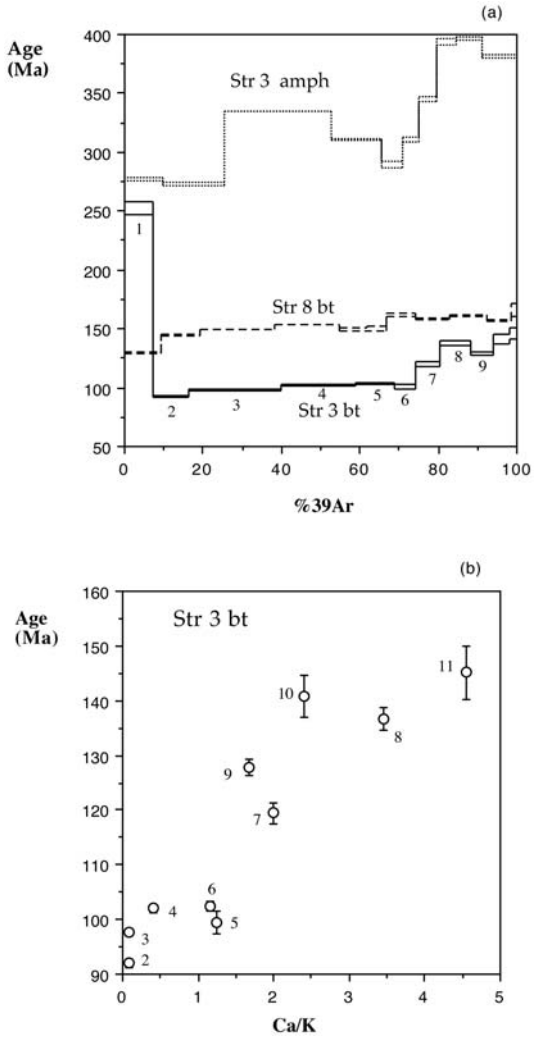

Fig. 15a, b Results for samples STR 3 and STR 8 (Saponara Subunit). Sample STR 3 was collected 5 km WSW from the strongly overprinted Badiazza area (which give ages in the range 50–60 Ma, see Fig. 8). **a** Age spectra of amphibole and biotites. **b** Ca/K age correlation diagram for biotites. The diagram reveals a mixing of two Ar reservoirs, only one of which is Ca-free. We identify it with the true mica and assign it an age of 95±3 Ma

Discussion

The results we obtained are complex and it is important to stress that our interpretations must be hierarchically structured. The foremost observation is that the age distribution along the SW–NE transect (Fig. 16) ranges from Proterozoic to Eocene. These age heterogeneities, which are present even inside what previously was considered as a single unit, characterise a sector which, up to now, was considered geochronologically uniform.

The basic interpretation of these data is that the entire orogenic edifice was formed in Hercynian times. Nappe stacking and peak metamorphic conditions are unquestionably and conclusively Hercynian. Pre-Hercynian relics are locally preserved. Alpine metamorphic paragneses are absent; the Alpine influence is limited to spatially very restricted, low-grade overprints.

Further, detailed interpretations of individual samples, and refinements to the broad picture just laid out, are open to improvement by further detailed work. Our samples reveal for the first time a heretofore unknown, very complex behaviour and it is hoped that future technical developments will allow greater resolution. We believe that closer ties between ever-improving electron microprobe data and geochronology will result in most reliable interpretations.

Proterozoic ages were recorded in the Cumia subunit. Amphiboles are interpreted as a mixture between a younger generation formed around 600 Ma and older cores. Even older ages around 1.6–1.8 Ga are provided by U-Pb dating of titanite. The literature contains other Precambrian zircon ages from the Peloritani-Aspromonte-Serre terrane (Schenk 1980). Our data show that the Proterozoic crust reworked by pre-Hercynian metamorphism extends as far south as the Peloritani Mountains.

"Eo-Hercynian" ages (350–420 Ma) were recorded in mafic amphibolites of the Mela Unit and of the Saponara Subunit. These tectonic (sub)units are interpreted as pre-Hercynian magmatic cumulates partly preserved from the complete Hercynian age overprint.

Hercynian ages (300–340 Ma) are recorded both in the Mela and Aspromonte Units. The younger (ca. 300 Ma) amphiboles from the Mela Unit are possibly related to the retrograde metamorphism, which affected the peak parageneses (cpx+grt).

A late-Hercynian (301±2 Ma) muscovite age was obtained from a mylonitic augengneiss marking the thrust contact between the Aspromonte Unit and the underlying lower-grade Mandanici Unit. Tertiary reactivation of Hercynian thrusts did not produce any rejuvenation of white micas in our study area.

Mesozoic ages were not recorded by amphiboles. Mica ages in the range 100–206 Ma were obtained both in the Mela and the Aspromonte Unit. Biotites mostly gave ages in the range 130–170 Ma, without a clear regional pattern. One pegmatite from the Saponara Gneiss Subunit gave concordant Rb-Sr and ^{39}Ar-^{40}Ar ages (203 Ma on muscovite, 139 Ma on biotite). The K-Ar-Rb-Sr concordance requires these ages to be interpreted as formation ages.

We propose that this cluster of biotite ages mirrors a period of intense hydrothermal activity between the Late Triassic and the Late Jurassic. Several hydrothermal events of similar age (e.g. Boni et al. 2001) are widespread elsewhere in the Southern Hercynides, e.g. Pyrenees, Catalunya, Sardinia, Serie dei Laghi.

Tertiary ages Eocene ages (48–61 Ma) were only found in micas from a very limited area of the Badiazza subunit.

It is important to note that less than 5 km westwards of Badiazza, biotite STR 3 is much less rejuvenated (100 Ma), while less than 4 km southwards of Badiazza we have found the Precambrian ages (Cumia). These observations show that the Tertiary event is very localised

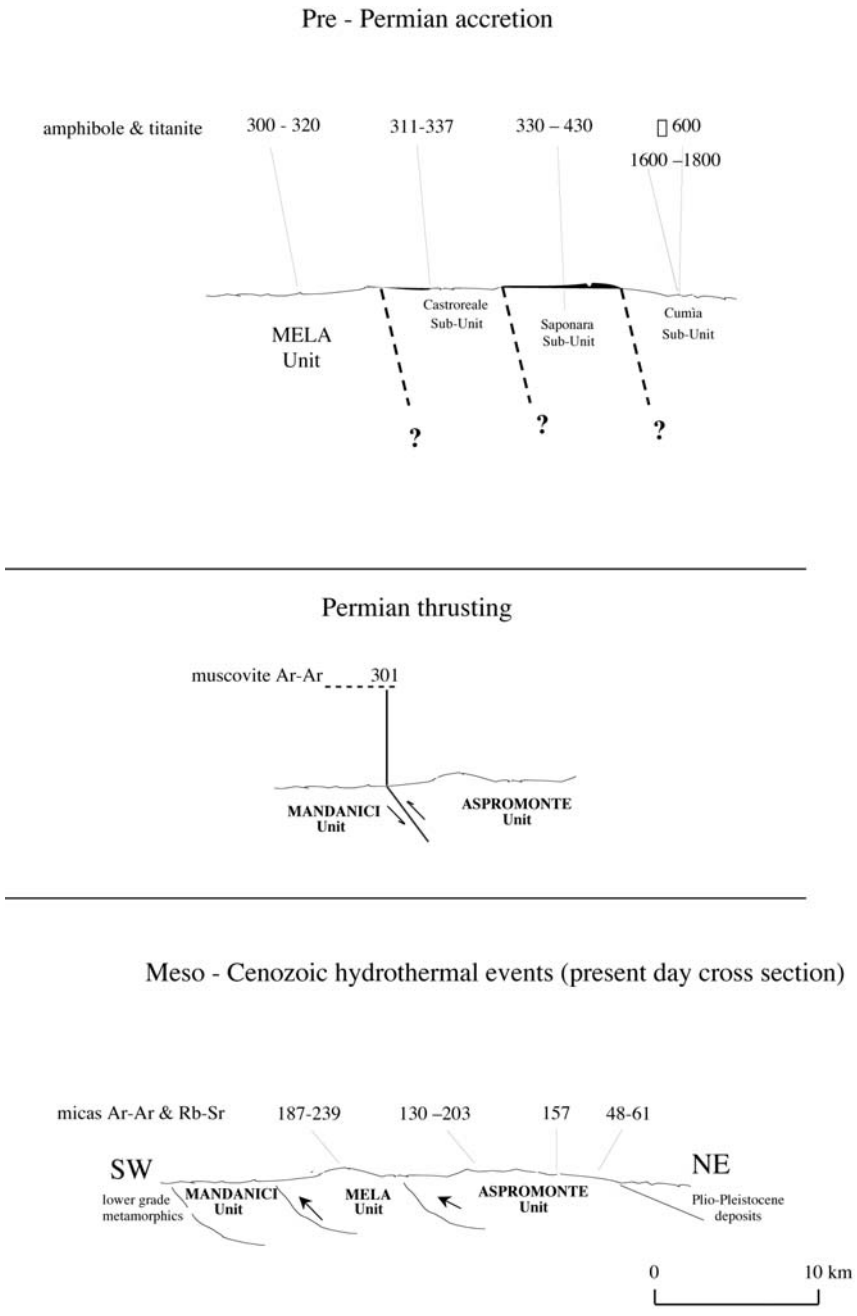

Fig. 16 Hypothetical N–S section showing the age results (Ma) across the Peloritani Mts. in a three-step evolutive scheme. Amphiboles were dated using the Ar-Ar method, micas by the Ar-Ar and Rb-Sr, titanite by the U-Pb method

along narrow shear zones characterised by a high strain rate (cf. Platt and Compagnoni 1990).

Conclusions

1. A 301±2 Ma age was obtained by ^{39}Ar-^{40}Ar on a muscovite from a mylonitic gneiss from the Aspromonte Unit at the tectonic contact with the underlying Mandanici Unit. This suggests that the orogen was mainly built in the Paleozoic. The presence of unmetamorphosed or very low-grade Meso-Cenozoic thin (and rare) sedimentary slices between these two units does not conflict with this observation, as it simply indicates a limited degree of Tertiary reactivation of older thrusts.
2. The geochronological heterogeneity of the Aspromonte "Unit" is an unexpected novelty. It derives from the welding of different pre-Hercynian and Hercynian terranes late during the Hercynian orogeny; the name "Unit" is no longer justified. We found multi-isotopic evidence for Proterozoic relics in the Cumia area.

In contrast with the well-preserved Aspromonte "Unit", the Mela Unit is characterised by: (a) pervasive retrogression, and (b) by generally younger ages. This could suggest that the Mela Unit underwent a different P–T evolution with respect to the Aspromonte "Unit" before both became welded in the Late Carboniferous.

3. During Triassic–Jurassic, both the Mela and Aspromonte "Units" underwent a hydrothermal event, which locally resulted in extensive recrystallisation of biotite and patchy recrystallisation of muscovite. This Triassic-Jurassic hydrothermal phase is also observed elsewhere in the Southern Hercynides.
4. The Tertiary overprint is present only in the Badiazza area, which is characterised by high strain rates and shear-induced recrystallisation.

Acknowledgements The first author acknowledges a grant from the University of Palermo enabling the sojourn in Bern. Isotope research in Bern was partly funded by SNF grant No. 20-6.00. Two anonymous reviewers and editorial remarks by K. Hammerschmidt helped to improve the manuscript.

Appendix

Table 5 shows Ar-Ar stepwise heating results.

References

Amodio Morelli L, Bonardi G, Colonna V, Dietrich D, Giunta G, Ippolito F, Liguori V, Lorenzoni S, Paglionico A, Perrone V, Piccarreta G, Russo AM, Scandone P, Zanettin-Lorenzoni E, Zuppetta A (1976) L' Arco Calabro-Peloritano nell' orogene Appenninico-Maghrebide. Mem Soc Geol It 17:1–60

Atzori P, Lentini F, Vezzani L, Lo Giudice A, Pezzino A (1975) Natura e significato dei lembi sedimentari interposti tra la falda dell' Aspromonte e la falda di Mandanici nei Monti Peloritani (Sicilia nord-orientale). Boll Soc Geol It 94:789–795

Atzori P, Del Moro, Rottura A (1990) Rb-Sr radiometric data from medium to high grade metamorphic rocks (Aspromonte nappe) of the north-eastern Peloritani Mountains (Calabrian Arc), Italy. Eur J Mineral 2:363–371

Atzori P, Cirrincione R, Del Moro A, Pezzino A (1994) Structural, metamorphic and geochronologic features of the Alpine event in the south-eastern sector of the Peloritani mountains (Sicily). Periodico Miner 63:113–125

Belluso E, Ruffini R, Schaller M, Villa IM (2000) Electron-microscope and Ar isotope characterization of chemically heterogeneous amphiboles from the Palala shear zone, Limpopo Belt, South Africa. Eur J Mineral 12:45–62

Bonardi G, Giunta G, Liguori V, Perrone V, Russo M, Zuppetta A (1976) Schema geologico dei Monti Peloritani. Boll Soc Geol Ital 95:49–74

Bonardi G, Compagnoni R, Del Moro A, Messina A, Perrone V (1987) Riequilibrazioni tettono-metamorfiche Alpine nell' Unità dell' Aspromonte Calabria meridionale. Rend Soc Ital Mineral Petrol 42:301

Boni M, Iannace A Villa IM, Fedele L, Bodnar R (2001) Multiple fluid-flow events and mineralizations in SW Sardinia: from Variscan onwards. In: Cidu R (ed) Water—rock interaction. Balkema, Lisse, pp 673–676

Borghi A, Compagnoni R, Messina A (1995) Prima segnalazione di un metamorfismo pre-alpino in facies eclogitica nell'arco Calabro-Peloritano. Plinius 14:74–75

Cirrincione R, Pezzino A (1991) Caratteri strutturali dell' evento alpino nella serie mesozoica di Alì e nella Unità metamorfica di Mandanici (Peloritani orientali) Mem Soc Geol Ital 47:263–272

Cirrincione R, Pezzino A (1994) Nuovi dati sulle succesioni Mesozoiche metamorfiche dei M. Peloritani orientali. Boll Soc Geol Ital 113:195–203

Compagnoni R, Borghi A, Messina A, Nutarelli F (1998) Metamorfismo eclogitico nell' Arco Calabro-Peloritano: un evento Varisico precoce o pre-Varisico ? Proc 79th Symp Soc Geol Ital Palermo 2:325–326

Krogh TE, Davis GL (1973). The effect of regional metamorphism on U-Pb systems in zircon and a comparison with Rb-Sr systems in the same whole rock and its constituent minerals. Carnegie Inst Wash Year Book 72, pp 601–610

Del Moro A, Pardini G, Maccarrone E, Rottura A(1982) Studio radiometrico Rb-Sr di granitoidi peraluminosi dell' Arco Calabro-Peloritano. Rend Soc Ital Mineral Petrol 38:1015–1026

Ferla P (1972) Serie metamorfiche dei M. Peloritani occidentali (Messina). Rend Soc Ital Mineral Petrol 28:125–151

Ferla P (1974) Aspetti petrogenetici e strutturali del polimetamorfismo dei M. Peloritani (Sicilia). Periodico Miner 43:517–590

Ferry JM, Spear FS (1978) Experimental calibration of the partitioning of Fe and Mg between biotite and garnet. Contrib Mineral Petrol 66:113–117

Frei R, Villa IM, Kramers JD, Nägler T, Przybylowicz WJ, Prozesky VM, Hofmann B, Kamber BS (1997) Single mineral dating by the Pb-Pb step-leaching method: assessing the mechanisms. Geochim Cosmochim Acta 61:393–414

Geyh MA, Schleicher H (1990) Absolute age determination: physical and chemical dating methods and their application. Springer, Berlin Heidelberg New York, 50 pp

Graham CM, Powell R (1984) A garnet-hornblende geothermometer: calibration, testing and application to the Pelona schists, southern California. J Metamorph Petrol 2:12–31

Holland T, Blundy J (1994) Non-ideal interactions in calcic amphiboles and their bearing on amphibole-plagioclase thermometry. Contrib Mineral Petrol 116:433–447

Indares A, Martignole J (1985) Biotite-garnet geothermometry in the granulite facies: the influence of Ti and Al in biotite. Am Mineral 70:272–278

Kretz R (1983) Symbols for rock forming minerals. Am Mineral 68:277–279

Krogh TE, Davis GL (1973) The effect of regional metamorphism on U-Pb systems in zircon and a comparison with Rb-Sr systems in the same whole rock and its constituent minerals. Carnegie Inst Wash Year Book 72:601–610

Ludwig KR (2000) User's manual for Isoplot/Ex, Version 22. A geochronological toolkit for Microsoft Excel. Berkeley Geochronology Center Spec Publ 1a, pp 1–53

Massonne HJ, Schreyer (1987) Phengite geobarometry based on the limiting assemblage with K-feldspar, phlogopite, and quartz. Contrib Mineral Petrol 96:212–224

Messina A (1998a) The Alpine Peloritani building (Calabria-Peloritani Arc). Proc 79th Soc Geol Ital Symp. Palermo 1998:565–568)

Messina A (1998b) Variscan tecto-metamorphic evolution in the crystalline basements of the Peloritani Mts. (Calabria-Peloritani Arc). Proc 79th Soc Geol Ital Symp. Palermo 1998:569–572

Messina A, Compagnoni R, Russo S, De Francesco AM, Giacobbe A (1990) Alpine metamorphic overprint in the Aspromonte nappe of northeastern Peloritani Mts (Calabria-Peloritani Arc, southern Italy). Boll Soc Geol Ital 109:655–673

Messina A, Perrone V, Giacobbe A, De Francesco AM (1997) The Mela Unit: a medium grade metamorphic unit in the Peloritani mountains (Calabria-Peloritani Arc, Italy). Boll Soc Geol Ital 116:237–252

Müller W, Kelley SP, Villa IM (2002) Dating fault-generated pseudotachylites: comparison of $^{40}Ar/^{39}Ar$ stepwise-heating,

laser-ablation and Rb/Sr microsampling analyses. Contrib Mineral Petrol 144:57–77
Ogniben L (1960) Nota illustrativa allo schema geologico della Sicilia nord-orientale. Riv Min Sic 64/65:183–212
Onstott TC, Miller ML, Ewing RC, Walsh D (1995) Recoil refinements: implications for the $^{40}Ar/^{39}Ar$ dating technique. Geochim Cosmochim Acta 59:1821–1834
Paglionico A, Piccarreta G (1978) History and petrology of a fragment of a fragment of deep crust in the Serre (Calabria, southern Italy). Neues Jahrb Miner Abh Mh 9:385–396
Pettke T, Diamond LW (1997) Oligocene gold quartz veins at Brusson, Western Alps: Sr isotopes trace the source of ore-bearing fluid to a 10-km depth. Econ Geol 92:389–406
Platt JP, Compagnoni R (1990) Alpine ductile deformation and metamorphism in a Calabrian basement nappe (Aspromonte, southern Italy). Eclog Geol Helv 83:41–58
Rotolo SG, De Fazio P (2001) Clinopyroxene-bearing garnet amphibolites from the Ferrà Valley (northern Peloritani Mts, Sicily). Boll Soc Geol Ital 120:31–35
Rottura A, Bargossi GM, Caironi V, Del Moro A, Maccarrone E, Macera P, Paglionico A, Petrini R, Piccarreta G, Poli G (1990) Petrogenesis of contrasting Hercynian granitoids from the Calabrian Arc, southern Italy. Lithos 24:97–119
Schenk V (1980) U-Pb and Rb-Sr radiometric dates and their correlation with metamorphic events in the granulite-facies basement of the Serre, southern Calabria. Contrib Mineral Petrol 73:23–38
Schenk V (1984) Petrology of felsic granulites, metamelites, metabasics, ultramafics, and metacarbonates from southern Calabria (Italy): prograde metamorphism, uplift and cooling of a former lower crust. J Petrol 25:255–298
Villa IM (2001) Radiogenic isotopes in fluid inclusions. Lithos 55:115–124
Villa IM, Hermann J, Müntener O, Trommsdorff V (2000) ^{39}Ar-^{40}Ar dating of multiply zoned amphibole generations (Malenco, Italian Alps). Contrib Mineral Petrol 140:363–381
Winter JD (2001) An introduction to igneous and metamorphic petrology. Prentice Hall, Englewood Cliffs, 697 pp
Zuppetta A, Russo M, Capaldi G, Tuccillo L (1984) Evidenze di un evento tettonico triassico nell' Unità dei Borghi (Monti Peloritani- Sicilia). Boll Soc Geol Ital 103:87–95